Measurement of the polarisation of W bosons produced with large transverse momentum in pp collisions at √s = 7 TeV with the ATLAS experiment

Aad, G.; et al., [Unknown]; Bentvelsen, S.; Colijn, A.P.; de Jong, P.; de Nooij, L.; Doxiadis, A.D.; Garitaonandia, H.; Geerts, D.A.A.; Gosselink, M.; Kayl, M.S.; Koffeman, E.; Lee, H.; Linde, F.; Mechnich, J.; Mussche, I.; Ottersbach, J.P.; Rijpstra, M.; Ruckstuhl, N.; Tsiakiris, M.; van der Kraaij, E.; van der Leeuw, R.; van der Poel, E.; van Kesteren, Z.; van Vulpen, I.; Vermeulen, J.C.; Vreeswijk, M.

Link to publication

Regular Article - Experimental Physics

Measurement of the polarisation of *W* bosons produced with large transverse momentum in *pp* collisions at $\sqrt{s} = 7$ TeV with the ATLAS experiment

The ATLAS Collaboration[*]

CERN, 1211 Geneva 23, Switzerland

Abstract This paper describes an analysis of the angular distribution of $W \rightarrow e\nu$ and $W \rightarrow \mu\nu$ decays, using data from *pp* collisions at $\sqrt{s} = 7$ TeV recorded with the AT-LAS detector at the LHC in 2010, corresponding to an integrated luminosity of about 35 pb^{-1}. Using the decay lepton transverse momentum and the missing transverse momentum, the *W* decay angular distribution projected onto the transverse plane is obtained and analysed in terms of helicity fractions f_0, f_L and f_R over two ranges of *W* transverse momentum (p_T^W) : $35 < p_T^W < 50$ GeV and $p_T^W > 50$ GeV. Good agreement is found with theoretical predictions. For $p_T^W > 50$ GeV, the values of f_0 and $f_L - f_R$, averaged over charge and lepton flavour, are measured to be: $f_0 = 0.127 \pm 0.030 \pm 0.108$ and $f_L - f_R = 0.252 \pm 0.017 \pm 0.030$, where the first uncertainties are statistical, and the second include all systematic effects.

1 Introduction

This paper describes a measurement with the ATLAS detector of the polarisation of *W* bosons with transverse momenta greater than 35 GeV, using the electron and muon decay modes, in data recorded at 7 TeV centre-of-mass energy, with a total integrated luminosity of about 35 pb^{-1}. The results are compared with theoretical predictions from MC@NLO [1] and POWHEG [2–5].

The paper is organised as follows. Section 2 describes the theoretical framework of this analysis. Section 3 reviews the relevant components of the ATLAS detector, the data, the corresponding Monte Carlo simulated data sets, and the event selection. The estimation of backgrounds after this selection is explained in Sect. 4, and the comparison of data and Monte Carlo simulations for the most relevant variable

$(\cos\theta_{2D})$ is given in Sect. 5. The construction of helicity templates and its validation using Monte Carlo samples is described in Sect. 6, while the uncorrected results are given in Sect. 7. The systematic uncertainties associated with the fitting procedure are discussed in Sect. 8 and the final results, corrected for reconstruction effects, are given in Sect. 9. Section 10 is devoted to the conclusions.

2 Theoretical framework and analysis procedure

Measuring the polarisation of particles is crucial for understanding their production mechanisms.

At hadron colliders, *W* bosons with small transverse momentum are mainly produced through the leading order electroweak processes

$$u\bar{d} \rightarrow W^+ \quad \text{and} \quad d\bar{u} \rightarrow W^-$$

At the LHC the quarks generally carry a larger fraction of the momentum of the initial-state protons than the antiquarks. This causes the *W* bosons to be boosted in the direction of the initial quark. In the massless quark approximation, the quark must be left-handed and the antiquark right-handed. As a result the *W* bosons with large rapidity (y_W) are purely left-handed.

For more centrally produced *W* bosons, there is an increasing probability that the antiquark carries a larger momentum fraction than the quark, so the helicity state of the *W* bosons becomes a mixture of left- and right-handed states whose proportions are respectively described with fractions f_L and f_R.

For *W* bosons with large transverse momentum, three main processes contribute (taking the W^+ as example):

$$ug \rightarrow W^+ d, \qquad u\bar{d} \rightarrow W^+ g \quad \text{and} \quad g\bar{d} \rightarrow W^+ \bar{u}$$

[*]e-mail: atlas.publications@cern.ch

Given the vector nature of the gluon, present in all three reactions, the simple argument used at low p_T^W no longer applies. Predictions require detailed helicity state calculations. Leading-order (LO) and next-to-leading-order (NLO) QCD predictions have been available for $p\bar{p}$ interactions for some time [6] and more recently for proton-proton interactions [7]. At high transverse momenta more complex production mechanisms contribute, and polarisation in longitudinal states is also possible (the proportion of longitudinal W bosons is hereafter described by f_0). This state is particularly interesting as it is directly connected to the massive character of the gauge bosons.

2.1 Theoretical framework

The general form for inclusive W production followed by its leptonic decay can be written as [6]:

$$\frac{d\sigma}{d(p_T^W)^2 \, dy_W \, d\cos\theta \, d\phi}$$

$$= \frac{3}{16\pi} \frac{d\sigma^u}{d(p_T^W)^2 \, dy_W} \times \Bigg[\left(1 + \cos^2\theta\right)$$

$$+ \frac{1}{2} A_0 \left(1 - 3\cos^2\theta\right) + A_1 \sin 2\theta \cos\phi$$

$$+ \frac{1}{2} A_2 \sin^2\theta \cos 2\phi + A_3 \sin\theta \cos\phi$$

$$+ A_4 \cos\theta + A_5 \sin^2\theta \sin 2\phi$$

$$+ A_6 \sin 2\theta \sin\phi + A_7 \sin\theta \sin\phi \Bigg] \quad (1)$$

where σ^u is the unpolarised cross-section and ϕ and θ are the azimuthal and polar angles of the charged lepton in a given W rest frame. The A_i coefficients are functions of p_T^W and y_W and depend on the parton distribution functions (PDFs). For $p_T^W \to 0$ all reference frames used in [6–12] become identical, with the z-axis directed along the beam axis. In these conditions the dependence on ϕ disappears and only the term with $(1 + \cos^2\theta)$ and the terms proportional to A_0 and A_4 remain.

The A_0 to A_4 coefficients in Eq. (1) receive contributions from QCD at leading and higher orders, while A_5 to A_7 appear only at next-to-leading order. Their expression as a function of p_T^W and y_W depends on the reference frame used for the calculation.

Several papers have been published to discuss and predict these coefficients, first for $p\bar{p}$ colliders [6, 8–12] and more recently for the LHC [7]. While at $p\bar{p}$ colliders, because of CP invariance, the A_i coefficients are either equal (A_0, A_2, A_3, A_5, A_7) or opposite (A_1, A_4, A_6) for W^+ and W^- production, there is no such simple relationship at pp colliders. However it has been observed [7] that A_3 and A_4

change sign between W^+ and W^-, while the other coefficients ($A_0, A_1, A_2, A_5, A_6, A_7$) do not and are similar in magnitude between W^+ and W^-. In all cases, the pure NLO coefficients (A_5 to A_7) are small. They are neglected in this analysis.

Experimental measurements have been reported from the Tevatron by CDF [13], from HERA by H1 [14] and recently from the LHC by CMS [15].

2.2 Helicity fractions

Helicity is normally measured by analysing the distribution of the cosine of the helicity angle (θ_{3D} in the following), defined as the angle between the direction of the W in the laboratory frame and the direction of the decay charged lepton in the W rest frame. The distribution of this angle as generated by MC@NLO is shown in Fig. 1 without phase space restriction, as well as with the acceptance (p_T^ℓ, η_ℓ and p_T^ν)[1] and W transverse mass m_T^W cuts (where $m_T^W = \sqrt{2(p_T^\ell p_T^\nu - \overrightarrow{p}_T^\ell \cdot \overrightarrow{p}_T^\nu)}$), described in Sect. 3.4.

The differential cross-section in the helicity frame[2] is expressed by using θ_{3D} and ϕ_{3D} in Eq. (1). Integrated over y_W and ϕ_{3D}, Eq. (1) then takes the form:
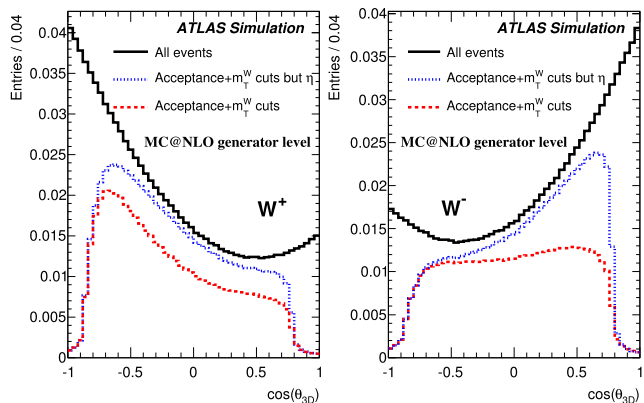
Fig. 1 Cosine of the helicity angle of the lepton from W decay at generator-level for positive charge (*left*) and negative charge (*right*). *Solid lines* are without selection, *dashed lines* are after all acceptance plus m_T^W cuts except the η_ℓ cuts and *dotted lines* are after all acceptance plus m_T^W cuts. "All events" distributions are normalised to unity

---

[1] ATLAS uses a right-handed coordinate system with its origin at the nominal interaction point (IP) in the centre of the detector and the z-axis along the beam pipe. The x-axis points from the IP to the centre of the LHC ring, and the y-axis points upward. Cylindrical coordinates (r, ϕ) are used in the transverse plane, ϕ being the azimuthal angle around the beam pipe. The pseudorapidity is defined in terms of the polar angle θ as $\eta = -\ln\tan(\theta/2)$.

[2] The helicity frame is the W rest frame with the z-axis along the W laboratory direction of flight and the x-axis in the event plane, in the hemisphere opposite to the recoil system.

$$\frac{1}{\sigma}\frac{d\sigma}{d\cos\theta_{3D}} = \frac{3}{8}\bigg[(1+\cos^2\theta_{3D}) + A_0\frac{1}{2}(1-3\cos^2\theta_{3D})$$

$$+ A_4\cos\theta_{3D}\bigg] \qquad (2)$$

Comparing Eq. (2) to the standard form [16] using helicity fractions:

$$\frac{1}{\sigma}\frac{d\sigma}{d\cos\theta_{3D}} = \frac{3}{8}f_L(1\mp\cos\theta_{3D})^2 + \frac{3}{8}f_R(1\pm\cos\theta_{3D})^2$$

$$+ \frac{3}{4}f_0\sin^2\theta_{3D} \qquad (3)$$

yields the relations between the A_i coefficients and the helicity fractions:

$$f_L(y_W, p_T^W) = \frac{1}{4}\big(2 - A_0(y_W, p_T^W) \mp A_4(y_W, p_T^W)\big)$$

$$f_R(y_W, p_T^W) = \frac{1}{4}\big(2 - A_0(y_W, p_T^W) \pm A_4(y_W, p_T^W)\big) \qquad (4)$$

$$f_0(y_W, p_T^W) = \frac{1}{2}A_0(y_W, p_T^W)$$

where the upper (lower) sign corresponds to W^+ (W^-) boson production respectively. It is interesting to notice that the difference between the left- and right-handed fraction is proportional to A_4 only, as:

$$f_L - f_R = \mp\frac{A_4}{2} \qquad (5)$$

From general considerations, the longitudinal helicity fraction f_0 is expected to vanish for $p_T^W \to 0$ as well as for $p_T^W \to \infty$, with a maximum expected around 45 GeV [7].

2.3 Analysis principle and variable definitions

When analysing data, a major difficulty arises from the incomplete knowledge of the neutrino momentum. The large angular coverage of the ATLAS detector enables measurement of the missing transverse momentum, which can be identified with the transverse momentum of the neutrino. The longitudinal momentum can be obtained through the W mass constraint. However, solving the corresponding equation leads to two solutions, between which it is not possible to choose in an efficient way. The approach taken in this analysis is to work in the transverse plane only, using the "transverse helicity" angle θ_{2D} defined by:

$$\cos\theta_{2D} = \frac{\vec{p}_T^{\ell*} \cdot \vec{p}_T^W}{|\vec{p}_T^{\ell*}||\vec{p}_T^W|} \qquad (6)$$

where $\vec{p}_T^{\ell*}$ is the transverse momentum of the lepton in the transverse W rest frame and $\vec{p}_T^W$ is the transverse momentum of the W boson in the laboratory frame. The angle θ_{2D}
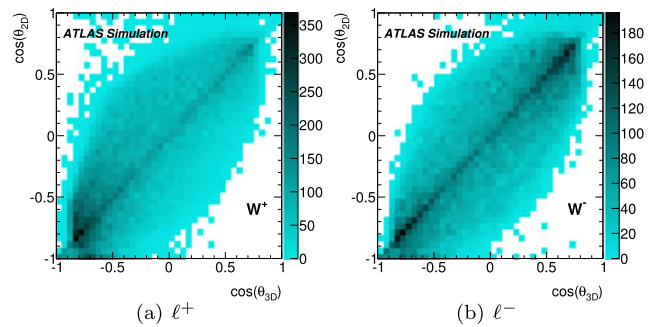
Fig. 2 Representation of $\cos\theta_{2D}$ as a function of $\cos\theta_{3D}$ in events where the W transverse momentum is greater than 50 GeV, for (**a**) positive and (**b**) negative leptons. Events are simulated with MC@NLO after applying the acceptance and m_T^W cuts, as defined in Sect. 3.4

is a two dimensional projection of the helicity angle θ_{3D}. Its determination uses only fully measurable quantities, defined in the transverse plane. Its use is limited to sizeable values of p_T^W, which corresponds to the physics addressed in this work.

The correlations between $\cos\theta_{2D}$ and $\cos\theta_{3D}$ for events where $p_T^W > 50$ GeV are represented in Figs. 2(a) and 2(b) for positive and negative leptons respectively. This information is obtained using a sample of events simulated with MC@NLO after applying acceptance and m_T^W cuts.

The enhancement near -1 for positive leptons reflects that the maximum of the left-handed part of the decay distribution (first term in Eq. (3)) falls within detector acceptance, as opposed to the case of negative leptons where the maximum (near $+1$) falls largely beyond the η_ℓ acceptance, resulting in a more "symmetric" distribution between forward and backward hemispheres. This effect is also seen in Fig. 1 when comparing $\cos\theta_{3D}$ distributions at generator-level, before and after the lepton pseudorapidity cut.

The measurement of helicity fractions is made by fitting $\cos\theta_{2D}$ distributions with a weighted sum of templates obtained from Monte Carlo simulations, which correspond to longitudinal, left- and right-handed states. This is described in detail in Sect. 6.

3 Detector, data and simulation

3.1 The ATLAS detector

The ATLAS detector [17] at the LHC covers nearly the entire solid angle around the collision region. It consists of an inner tracking system surrounded by a thin superconducting solenoid, electromagnetic and hadronic calorimeters, and a muon spectrometer incorporating three large superconducting toroid magnets.

The inner detector (ID) is immersed in a 2 T axial magnetic field and allows charged particle tracking in the range

$|\eta| < 2.5$. The high-granularity silicon pixel detector covers the vertex region and typically provides three measurements per track. It is followed by the silicon microstrip tracker which usually provides four two-dimensional measurement points per track. These silicon detectors are complemented by the transition radiation tracker, which enables radially extended track reconstruction up to $|\eta| = 2.0$. The transition radiation tracker also provides electron identification information based on the fraction of hits (typically 30 per track) above an energy threshold corresponding to transition radiation.

The calorimeter system covers the pseudorapidity range $|\eta| < 4.9$. Within the region $|\eta| < 3.2$, electromagnetic calorimetry is based on barrel and end-cap high-granularity lead liquid-argon (LAr) electromagnetic calorimeters, with an additional thin LAr presampler covering $|\eta| < 1.8$ to correct for energy loss in material upstream of the calorimeters. Hadronic calorimetry is provided by a steel/scintillating-tile detector, segmented into three structures within $|\eta| < 1.7$, and two copper/LAr hadronic endcap calorimeters. The solid angle coverage is completed with forward copper/LAr and tungsten/LAr calorimeter modules optimised for electromagnetic and hadronic measurements respectively.

The muon spectrometer (MS) comprises separate trigger and high-precision tracking chambers measuring the deflection of muons in a magnetic field generated by superconducting air-core toroids. The precision chamber system covers the region $|\eta| < 2.7$, with three layers of monitored drift tubes complemented by cathode strip chambers in the region beyond $|\eta| = 2.0$ where the background is highest. The muon trigger system covers the range $|\eta| < 2.4$ with resistive plate chambers in the barrel, and thin gap chambers in the endcap regions.

A three-level trigger system is used to select interesting events [18]. The Level-1 trigger is implemented in hardware and uses a subset of detector information to reduce the event rate to a design value of at most 75 kHz. This is followed by two software-based trigger levels which together reduce the event rate to about 200 Hz.

3.2 Data sample

The data used in this analysis were collected from August to October 2010. Requirements on beam, detector and trigger conditions, as well as on data quality, were used in the event selection, resulting in integrated luminosities of 37.3 pb^{-1} for the electron channel and 31.4 pb^{-1} for the muon channel (data where the muon trigger conditions varied too rapidly were not included).

The integrated luminosity measurement has an uncertainty of 3.4 % [19, 20].

3.3 Simulation

Signal and background samples were processed through a GEANT4 [21] simulation of the ATLAS detector [22] and reconstructed using the same analysis chain as the data.

The signal samples were generated using MC@NLO 3.4.2 with HERWIG [23] parton showering, and with POWHEG 1.0 and PYTHIA parton showering. Both used the CTEQ 6.6 [24] PDF set. All background samples were generated with PYTHIA 6.4.21 [25] except $t\bar{t}$ for which MC@NLO was used. In order to study the sensitivity of the angular distributions to different NLO PDF sets, the MC@NLO sample was reweighted [26] according to MSTW 2008 [27] and HERAPDF 1.0 [28] PDF sets.

The radiation of photons from charged leptons was simulated using PHOTOS [29], and TAUOLA [30] was used for τ decays. The underlying event [31] was simulated according to the ATLAS tune [32]. The Monte Carlo samples were generated with, in average, two soft inelastic collisions overlaid on the hard-scattering event. Events were subsequently reweighted so that the distribution of the number of reconstructed vertices matched that in data, which was 2.2 on average.

3.4 Event selection

Events in this analysis are first selected using either a single-muon trigger with a requirement on the transverse momentum p_{T}^{ℓ} of at least 13 GeV, or a single-electron trigger, with a p_{T}^{ℓ} requirement of at least 15 GeV [18]. Subsequent selection criteria closely follow those used for the W boson inclusive cross-section measurement reported in [33].

Events from pp collisions are selected by requiring a reconstructed vertex compatible with the beam-spot position and with at least three associated tracks each with transverse momentum greater than 0.5 GeV.

Electron candidates are required to satisfy $p_{\mathrm{T}}^{\ell} > 20$ GeV, $|\eta| < 2.47$ (but removing the region where barrel and end-cap calorimeters overlap, i.e. $1.37 < |\eta| < 1.52$) and to pass the "tight" identification criteria described in [34]. This selection rejects charged hadrons and secondary electrons from conversions by fully exploiting the electron identification potential of the detector. It makes requirements on shower shapes in the electromagnetic calorimeter, on the angular matching between the calorimeter energy cluster and the ID track, on the ratio of cluster energy to track momentum, and on the number of hits in the pixels (in particular a hit in the innermost layer is required), in the silicon microstrip tracker and in the transition radiation tracker.

Muon candidates are required to be reconstructed in both the ID and the MS, with transverse momenta satisfying the

conditions $|(p_T^{MS} - p_T^{ID})/p_T^{ID}| < 0.5$ and $p_T^{MS} > 10$ GeV. The two measurements are then combined, weighted by their respective uncertainties, to form a *combined muon*. The W candidate events are required to have at least one combined muon track with $p_T^\ell > 20$ GeV, within the range $|\eta| < 2.4$. This muon candidate must also satisfy the isolation condition $(\Sigma p_T^{ID})/p_T^\ell < 0.2$, where the sum is over all charged particle tracks around the muon direction within a cone of size $\Delta R = \sqrt{(\Delta\eta)^2 + (\Delta\phi)^2} = 0.4$. Finally, to reduce the contribution of cosmic-ray events, and beam-halo induced by proton losses from the beam, the analysis requires the reconstructed vertex position along the beam axis to be within 20 cm of the nominal interaction point.

The missing transverse momentum (E_T^{miss}) is reconstructed as the negative vector sum of calibrated "objects" (jets, electrons or photons, muons) to which the energies of calorimeter cells not associated to any of the objects are added. E_T^{miss} is required to be larger than 25 GeV. A cut $m_T^W > 40$ GeV is finally applied.

In addition to these cuts, called in the following *standard cuts*, additional selections are used for this analysis. A low m_T^W cut at 50 GeV is applied to minimise backgrounds, and a high m_T^W cut at 110 GeV is applied to remove tails of badly reconstructed events. Finally a p_T^W selection in two bins ($35 < p_T^W < 50$ GeV, and $p_T^W > 50$ GeV) is made. The numbers of events passing these cuts are shown in Table 1.

The data are compared to expectations based on Monte Carlo simulations. In addition to the signal (W production followed by leptonic decay to an electron or a muon), the following electroweak backgrounds are considered: $W \to \tau\nu$, $Z \to ee$, $Z \to \mu\mu$ and $Z \to \tau\tau$, as well as $t\bar{t}$ events with at least one semi-leptonic decay. Jet production via QCD was also simulated, but the final estimate of this background is obtained from data, as explained in Sect. 4.2.

4 Signal normalisation and background estimate

4.1 Signal normalisation

The $W^\pm \to \ell\nu$ production cross-sections and the decay branching ratios used in this study are normalised to the NNLO predictions of the FEWZ program [35] with the MSTW 2008 PDF set:

$$\sigma_{W^+ \to \ell\nu}^{NNLO} = 6.16 \text{ nb}$$

$$\sigma_{W^- \to \ell\nu}^{NNLO} = 4.30 \text{ nb}$$

The estimated uncertainties on each cross-section coming from the factorisation and renormalisation scales as well as from the parton distribution functions are expected to be approximately 5 % [33].

4.2 Background estimates

W events decaying into τ-leptons with subsequent leptonic τ decays contribute as background to both electron and muon channels. Contributions from $Z \to \mu\mu$ decays are significant in the muon channel, where the limited η coverage of the tracking and muon systems can result in fake E_T^{miss} when one of the muons is missed. On the contrary, the $Z \to ee$ background is almost negligible in the electron channel due to the nearly hermetic calorimeter coverage over $|\eta| < 4.9$. For both the electron and the muon channels, contributions from $Z \to \tau\tau$ decays and from $t\bar{t}$ events involving at least one leptonic W decay are also taken into account. The latter is particularly relevant for the large transverse momentum W bosons studied here.

The normalisation of electroweak and $t\bar{t}$ backgrounds is based on their total theoretical cross-sections. These cross-sections are calculated at NLO (plus next-to-next-to-leading-log corrections) for $t\bar{t}$ [36, 37], and at NNLO for the

Table 1 Numbers of events in data and signal Monte Carlo samples, after standard and analysis cuts (see text), classified according to lepton flavour and charge. The remaining numbers of events after standard plus analysis cuts are also represented as a percentage of the numbers of events passing the standard selection

		μ^+	μ^-	e^+	e^-
Data	Standard cuts	79713	52186	67130	45690
	Analysis cuts ($35 < p_T^W < 50$ GeV)	4459 (5.6 %)	3018 (5.8 %)	3778 (5.6 %)	2656 (5.8 %)
	Analysis cuts ($p_T^W \geq 50$ GeV)	3921 (4.9 %)	2640 (5.1 %)	3573 (5.3 %)	2572 (5.6 %)
MC@NLO	Standard cuts	1484062	1041818	1054705	774952
	Analysis cuts ($35 < p_T^W < 50$ GeV)	76807 (5.2 %)	52781 (5.1 %)	54044 (5.1 %)	39528 (5.1 %)
	Analysis cuts ($p_T^W \geq 50$ GeV)	57699 (3.9 %)	39114 (3.8 %)	43509 (4.1 %)	31283 (4.0 %)
POWHEG	Standard cuts	1498352	1056697	1056561	775894
	Analysis cuts ($35 < p_T^W < 50$ GeV)	82174 (5.5 %)	59788 (5.7 %)	58423 (5.5 %)	44276 (5.7 %)
	Analysis cuts ($p_T^W \geq 50$ GeV)	66674 (4.5 %)	47115 (4.6 %)	50705 (4.8 %)	37792 (4.9 %)

others. The contributions of these backgrounds to the final data sample have been estimated using simulation to model acceptance effects.

One of the major background contributions, especially in the electron channel, is from dijet production via QCD processes. The selected leptons from these processes have components from semi-leptonic decays of heavy quarks, hadrons misidentified as leptons, and, in the case of the electron channel, electrons from conversions. The missing transverse momentum is due mainly to jet mismeasurement. For both the electron and muon channels, these sources of background are obtained from the data. Monte Carlo simulated samples are also used for cross-checks.

The jet background is obtained by fitting the E_T^{miss} data distributions to the sum of the $W^\pm \to \ell \nu$ signal and the electroweak and $t\bar{t}$ backgrounds, normalised as described above and called hereafter the "electroweak template", plus a "jet event template" derived from control samples in the data.

In the electron case, the jet event template is obtained by selecting electron candidates passing the "loose" selection [34], but failing one or more of the additional criteria required to flag an electron as "medium" as well as an isolation cut (which removes signal events).

In the muon case, the jet event template is obtained by inverting the track isolation requirement.

In both cases, the relative normalisation of the jet event and electroweak templates is determined by fitting the two templates to the E_T^{miss} distribution in the data down to 10 GeV. The jet event fraction is then obtained from the (normalised) jet event template by counting events above $E_T^{miss} = 25$ GeV.

The background fractions determined with the methods described above, for the standard cuts and for the standard plus analysis cuts, are shown in Table 2. These results were obtained with MC@NLO for the signal simulation, and are in agreement with those obtained with POWHEG. For the muon channel, as jet event fractions are small and measured with larger uncertainties than for electrons, a value of 2 % with an uncertainty of ±2 % is used for both W^+ and W^-. Table 2 shows the statistical uncertainties from the jet template method. Uncertainties on the measurement due to background modelling are described in Sect. 8.1.

5 Data to Monte Carlo comparison of transverse helicity

As shown in [33], MC@NLO and POWHEG give a rather good description of inclusive W production. However both generators were shown [38] to underestimate the fraction of events at large p_T^W (see also Table 1). While this affects the relative fraction of data versus Monte Carlo events retained in the two p_T^W bins of the analysis, it should not significantly impact the angular distributions used to measure the W polarisation. This is discussed in more detail in Sect. 8.3.

Figures 3 and 4 show the $\cos\theta_{2D}$ distributions for electrons and muons and both charges, compared to the predictions from MC@NLO and POWHEG and to the expected behaviour of unpolarised W bosons (the unpolarised distributions are obtained by averaging the longitudinal, left- and right-handed MC@NLO templates with equal weights, see Sect. 6.1). The good agreement of

Table 2 Background fractions (with respect to the expected signal) obtained from Monte Carlo simulations (electroweak and $t\bar{t}$) normalised to state-of-the-art signal cross-section predictions (see text) and from data (jet background) by fitting E_T^{miss} distributions with templates

	Fractions (%)	μ^+	μ^-	e^+	e^-
Standard cuts	jet	2.1 ± 0.1	3.1 ± 0.2	2.4 ± 0.1	3.6 ± 0.1
	$t\bar{t}$	0.2	0.4	0.3	0.5
	$W \to \tau\nu$	2.6	2.8	2.3	2.5
	$Z \to \tau\tau$	0.1	0.2	0.1	0.1
	$Z \to \ell\ell$	2.9	3.9	0.1	0.2
Analysis cuts ($35 < p_T^W < 50$ GeV)	jet	2 ± 2	2 ± 2	2.4 ± 0.4	2.5 ± 0.5
	$t\bar{t}$	0.5	0.7	0.6	0.9
	$W \to \tau\nu$	2.1	2.4	1.8	1.9
	$Z \to \tau\tau$	0.1	0.1	0.1	0.1
	$Z \to \ell\ell$	2.9	3.9	0.3	0.4
Analysis cuts ($p_T^W > 50$ GeV)	jet	2 ± 2	2 ± 2	2.0 ± 0.3	2.5 ± 0.4
	$t\bar{t}$	2.8	4.1	3.5	5.0
	$W \to \tau\nu$	2.1	2.0	1.9	2.0
	$Z \to \tau\tau$	0.1	0.1	0.1	0.1
	$Z \to \ell\ell$	2.6	3.5	0.3	0.4

both the MC@NLO and POWHEG distributions with data is demonstrated also by the χ^2 values reported in Table 3. It is also clear from Table 3 and Figs. 3 and 4 that the production of unpolarised W bosons does not match the data.

For the electron channel, the jet background clusters around $\cos\theta_{2D} = 1$, which supports the assumption that these were two-jet events, where one of the jets was misidentified as an electron. On the other hand, in the muon channel, the jet background clusters around $\cos\theta_{2D} = -1$, in agreement with the assumption that the background origi-

nates mainly from semi-leptonic decay of heavy-flavour in jets.

6 Helicity templates and Monte Carlo closure test

6.1 Construction of helicity templates

In order to measure the helicity fractions, it is necessary to construct $\cos\theta_{2D}$ distributions corresponding to samples of longitudinal, left- and right-handed W bosons that decay

Fig. 3 The $\cos\theta_{2D}$ distributions for $35 < p_T^W < 50$ GeV. The data (*dots*) are compared to the distributions from POWHEG (*dashed line*), MC@NLO (*solid line*), and for unpolarised W bosons (*dotted line*) in the muon (*top*) and electron (*bottom*) channel, split by charge. The *bottom parts of each plot* represent the ratio of data, POWHEG and unpolarised distributions to MC@NLO
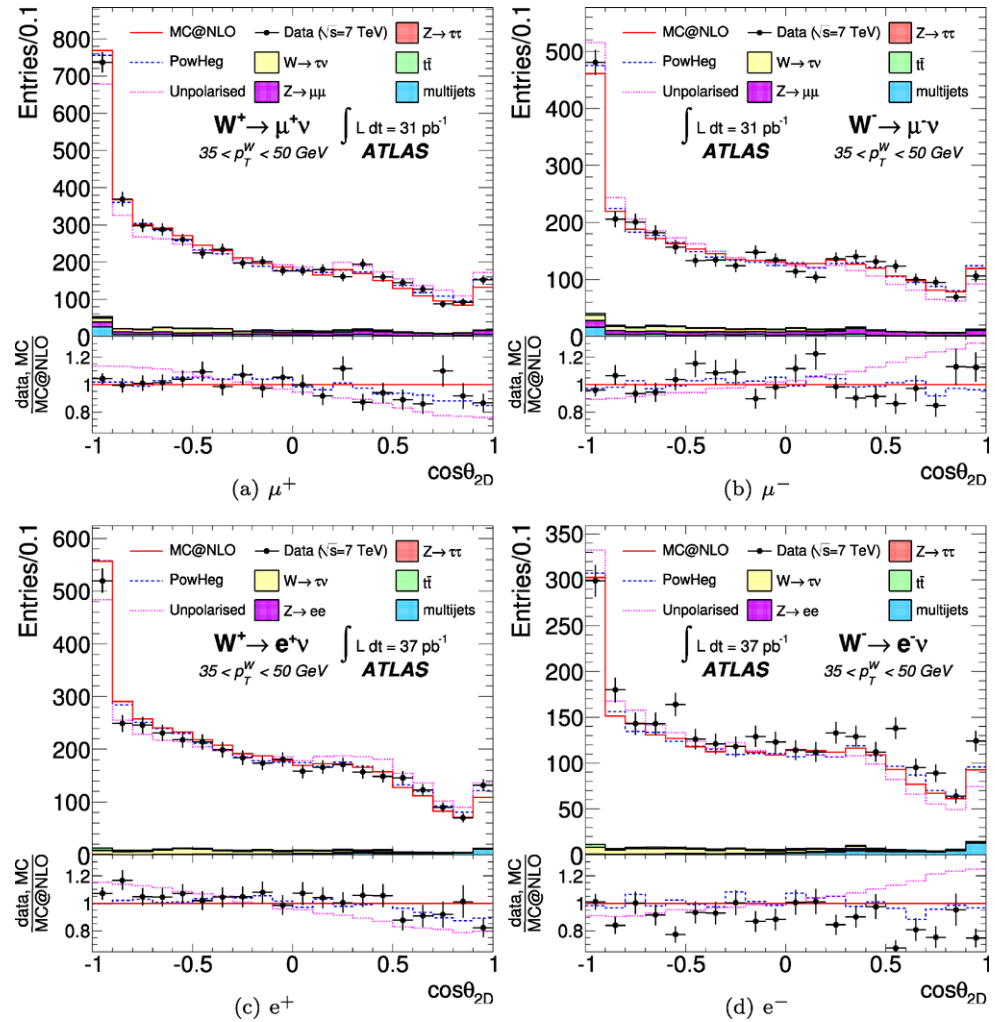
Table 3 The χ^2 values from the comparison of the data with the MC@NLO, POWHEG and unpolarised predictions for the $\cos\theta_{2D}$ distributions (see Figs. 3 and 4). The number of degrees of freedom in the fits is 19. Only statistical uncertainties are considered

χ^2 between data and	$35 < p_T^W < 50$ GeV				$p_T^W > 50$ GeV			
	μ^+	μ^-	e^+	e^-	μ^+	μ^-	e^+	e^-
MC@NLO Monte Carlo	20.0	25.0	17.0	32.1	36.2	31.5	28.6	17.3
POWHEG Monte Carlo	12.8	22.9	10.7	25.5	40.3	32.7	30.3	16.3
Unpolarised	23.6	33.5	28.0	79.5	62.4	44.2	129.2	42.9

Fig. 4 The $\cos\theta_{2D}$ distributions for $p_T^W > 50$ GeV. The data (*dots*) are compared to the distributions from POWHEG (*dashed line*), MC@NLO (*solid line*), and for unpolarised W bosons (*dotted line*) in the muon (*top*) and electron (*bottom*) channel, split by charge. The *bottom parts of each plot* represent the ratio of data, POWHEG and unpolarised distributions to MC@NLO

(a) μ^+

(b) μ^-

(c) e^+
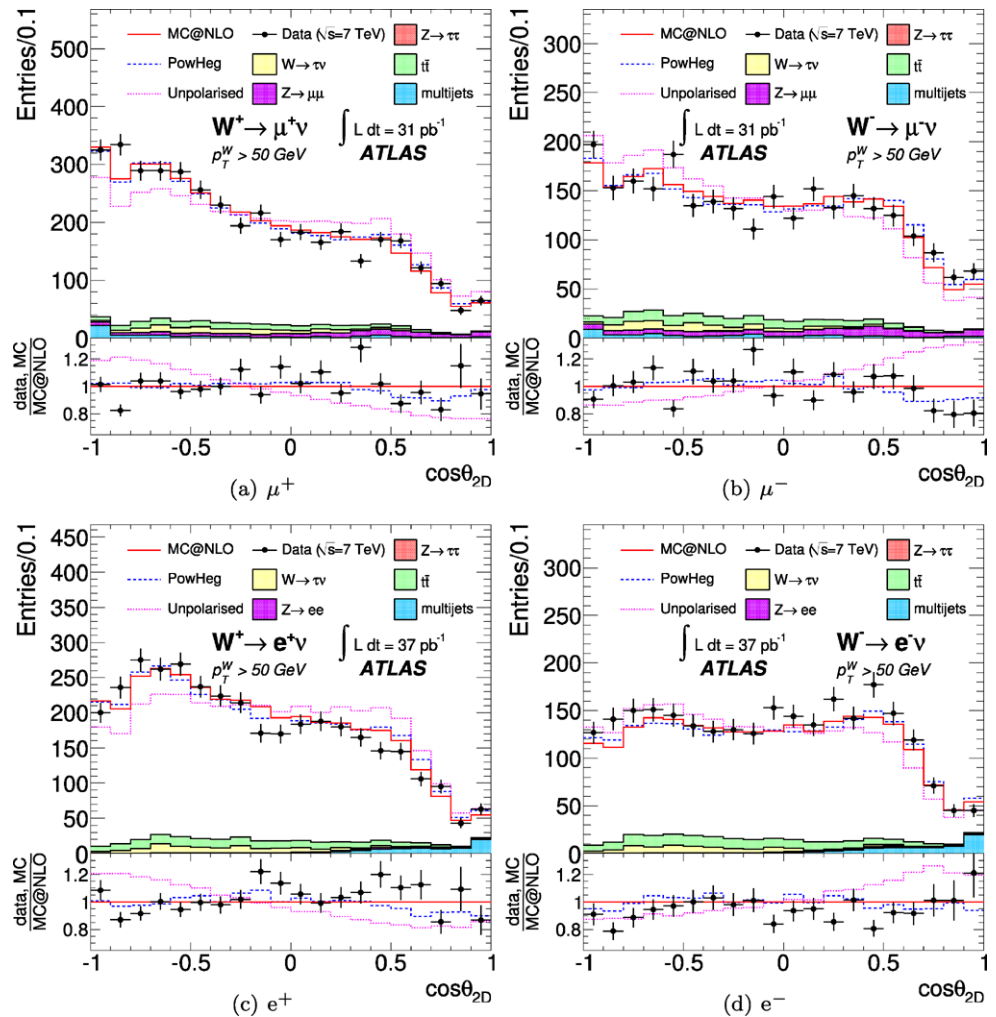
(d) e^-

into a lepton and a neutrino. As a check at the generator-level, and for the correction procedure (see Sect. 8.6), $\cos\theta_{3D}$ distributions corresponding to the three polarisation states were also made. All these distributions are called helicity templates in the following. The templates were built independently from MC@NLO and from POWHEG using the following reweighting technique.

It was first verified that, at the generator-level, and in bins of limited size in p_T^W and y_W, W decays generated with the Monte Carlo simulations are well described by Eq. (3). The generator-level $\cos\theta_{3D}$ distributions were then fitted with the distribution corresponding to this equation, which gave the values of f_L, f_0 and f_R in y_W and p_T^W bins. The results, in terms of f_0 and $f_L - f_R$, are shown in Fig. 5 for MC@NLO. The size of the bins results from a compromise between the rate of variation of the coefficients and the size of the available samples.

Several conclusions may be drawn from Fig. 5. The longitudinal fraction, which is very small for low p_T^W, grows with p_T^W (especially at low $|y_W|$), before flattening out and then starting to decrease. The difference between the frac-

tions of left- and right-handed W bosons is small for low $|y_W|$ and grows quickly with $|y_W|$, reaching up to 70 % for $|y_W| = 3$. As already explained in Sect. 1, a smaller left-right difference is expected for negative than for positive W bosons; however in the p_T^W range analysed here, these differences differ by at most a few percent. The analysis of systematic uncertainties described in Sect. 8.5, shows that it is experimentally advantageous to average the measured values of $f_L - f_R$ between the two charges. As an anticipation of this observation, it can be seen in Fig. 5 that this averaging is physically meaningful.

An equivalent analysis for POWHEG shows a similar trend for $f_L - f_R$ as observed for MC@NLO. For f_0, in the p_T^W range analysed here, POWHEG exhibits a much flatter dependence on y_W than MC@NLO, the average values being, however, very close to each other. Analytical calculations at NNLO reported in [7] by the BlackHat collaboration are very close to POWHEG. This is illustrated in Fig. 6.

Samples representing longitudinal, left- and right-handed states are obtained by reweighting the MC@NLO or POWHEG

Fig. 5 Computed values of f_0 (*top*) and $f_L - f_R$ (*bottom*) using fits with Eq. (3) to MC@NLO samples in ($|y_W|$, p_T^W) bins, split by charge. These values are used to calculate the weights needed to create helicity templates

(a) f_0 for ℓ^+

(b) f_0 for ℓ^-

(c) $f_L - f_R$ for ℓ^+

(d) $f_L - f_R$ for ℓ^-
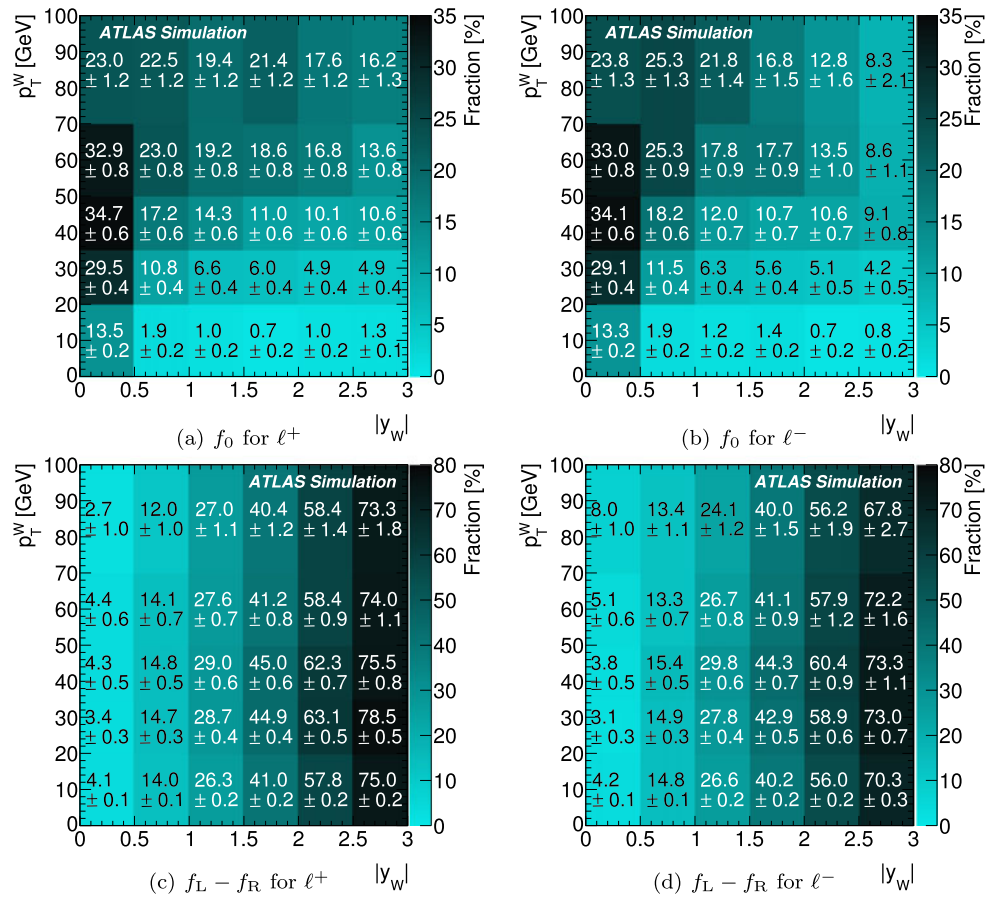
Fig. 6 Evolution of the longitudinal polarisation fraction as a function of $|y_W|$, in MC@NLO, POWHEG and a calculation based on BlackHat, for W^+ (*top*) and W^- (*bottom*) for two p_T^W bins
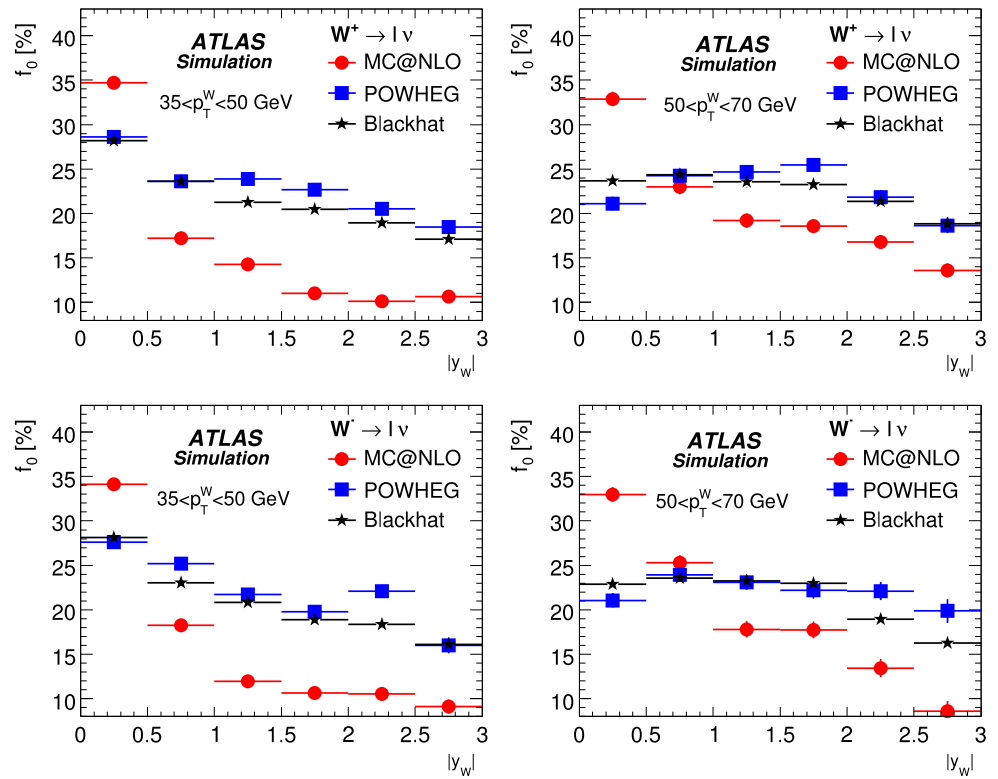
simulated events according to:

$$\frac{\frac{1}{\sigma^{\pm}}\frac{d\sigma^{\pm}}{d\cos\theta_{3D}}\big|_{L/0/R}}{\frac{3}{8}f_L(1\mp\cos\theta_{3D})^2+\frac{3}{8}f_R(1\pm\cos\theta_{3D})^2+\frac{3}{4}f_0\sin^2\theta_{3D}} \tag{7}$$

where

$$\frac{1}{\sigma^{\pm}}\frac{d\sigma^{\pm}}{d\cos\theta_{3D}}\bigg|_{\substack{L\\0\\R}}=\frac{3}{8}\begin{cases}(1\mp\cos\theta_{3D})^2\\2\sin^2\theta_{3D}\\(1\pm\cos\theta_{3D})^2\end{cases} \tag{8}$$

and where the denominator corresponds to the general form of the differential cross-section in which the coefficients are taken from Fig. 5 (or its equivalent from POWHEG), for the corresponding value of p_T^W and $|y_W|$. In these equations, the upper (lower) sign corresponds to W^+ (W^-) boson.

6.2 Fit procedure applied to Monte Carlo samples

The fitting procedure with templates was first applied to the simulated samples, at three different levels:

– all events using generator information for $\cos\theta_{3D}$ distributions;
– events remaining after applying acceptance and m_T^W cuts using generator information for $\cos\theta_{3D}$ distributions;
– events after the complete event selection (standard plus analysis cuts), using fully simulated information followed by reconstruction for $\cos\theta_{2D}$ distributions.

The fits of $\cos\theta_{3D}$ and $\cos\theta_{2D}$ distributions were performed using a binned maximum-likelihood fit [39, 40]. Since the parameters of the fit, f_0, f_L and f_R, must sum to 1, only two independent parameters, chosen to be f_0 and

$f_L - f_R$, are reported. The parameters were not individually constrained to be between 0 and 1.

For the second and third steps, numerical results for f_0 and $f_L - f_R$ fits are summarised in Table 4 for $35 < p_T^W < 50$ GeV and $p_T^W > 50$ GeV. In Table 4 and in the following, the coefficients f_0 and $f_L - f_R$ represent helicity fractions, averaged over y_W, within a given p_T^W bin.

Template fit results using the $\cos\theta_{3D}$ distributions at the generator-level, without any cut, reproduce the average value of the numbers quoted in the relevant p_T^W bin of Fig. 5. With respect to these fit results, the numbers shown in the first lines of Table 4 for the two p_T^W bins reflect the effect of the acceptance and m_T^W cuts, which is small on f_0 but is sizeable on $f_L - f_R$, typically reducing it by 25 % (relative). Indeed, the detector has a small acceptance for the events produced at high $|y_W|$, for which $f_L - f_R$ is largest.

Comparisons of the first row of each part of Table 4 ($\cos\theta_{3D}$ at generator-level, within acceptance) to the second row ($\cos\theta_{2D}$ after full simulation) indicates that the values of f_0 are rather stable for W^- while for W^+ there is in several cases a significant increase. Similar effects are observed with POWHEG. Corrections applied at the analysis level (see Sect. 8.6) are intended to remove these effects to obtain the final, corrected results.

7 Fit results

The raw helicity fractions for each of the four analysed channels were obtained by fitting the experimental $\cos\theta_{2D}$ distributions, after background subtraction, with a sum of templates (see Eq. (3)) corresponding to longitudinal, left- and right-handed states.

In order to correct for systematic effects associated with the choice of the variable used in the fit ($\cos\theta_{2D}$), and for

Table 4 Results (as percentages) of fitting $\cos\theta_{3D}$ and $\cos\theta_{2D}$ distributions from MC@NLO simulated samples using helicity templates. The fits are performed at generator-level, after applying acceptance and m_T^W cuts, and on fully simulated events, after applying standard plus analysis selections using $\cos\theta_{2D}$

		μ^+	μ^-	e^+	e^-
		$35 < p_T^W < 50$ GeV			
$\cos\theta_{3D}$ generator-level	f_0 (%)	14.6 ± 0.8	20.9 ± 0.8	15.3 ± 0.8	20.4 ± 0.9
	$f_L - f_R$ (%)	27.9 ± 0.7	26.5 ± 0.8	28.2 ± 0.7	26.4 ± 0.8
$\cos\theta_{2D}$ fully simulated	f_0 (%)	30.1 ± 2.4	19.5 ± 2.2	26.9 ± 2.2	21.6 ± 2.3
	$f_L - f_R$ (%)	31.8 ± 1.4	26.5 ± 1.2	27.3 ± 1.4	22.5 ± 1.4
		$p_T^W \geq 50$ GeV			
$\cos\theta_{3D}$ generator-level	f_0 (%)	18.3 ± 1.0	22.7 ± 1.0	19.0 ± 0.9	22.1 ± 1.0
	$f_L - f_R$ (%)	26.9 ± 0.8	25.8 ± 0.9	27.6 ± 0.8	25.9 ± 0.9
$\cos\theta_{2D}$ fully simulated	f_0 (%)	25.1 ± 1.9	20.7 ± 2.2	24.9 ± 1.8	22.5 ± 2.0
	$f_L - f_R$ (%)	29.7 ± 1.1	26.2 ± 1.2	25.6 ± 1.2	22.6 ± 1.3

resolution effects, the raw results have been corrected in a second step by the differences observed in Monte Carlo events between the fits at the generator level with the $\cos\theta_{3D}$ distribution after acceptance plus m_T^W cuts and the fit on $\cos\theta_{2D}$ distributions after full simulation. The two sets of templates obtained from MC@NLO or from POWHEG were used, and their bias corrected for accordingly. Differences between the results obtained with the two Monte Carlo generators were used to estimate a systematic uncertainty associated with the choice of templates (see Sect. 8.6).

The minimisation [39] gives the uncertainties and correlations between the parameters. The χ^2 values, in Table 5, obtained using MC@NLO and POWHEG templates, are similar. They are significantly lower, in most cases, than in Table 3, especially for muons, even taking into account that the number of degrees of freedom is reduced from 19 to 17.

The values of the fitted parameters, using MC@NLO and POWHEG templates, are reported in Table 6. The contributions of the individual fitted helicity states, and their sum, are also shown, for the MC@NLO case, in Fig. 7 for $35 < p_T^W <50$ GeV, and in Fig. 8 for $p_T^W > 50$ GeV. These histograms show the contributions of each polarisation state (separately and summed together), with a normalisation which, in addition to the value of f_0, f_L and f_R, also takes into account the relative average acceptance for each of the three polarisation states. The data show a dominance of the left-handed

over the right-handed fraction in about the same proportion as in the Monte Carlo simulations.

The f_0 values obtained with the POWHEG templates are in general larger (see Table 6). For the negative charges, the increase of f_0 is correlated with a decrease of $f_L - f_R$, while for positive charges the reverse is observed, though with a smaller increase, especially in the higher p_T^W bin.

8 Systematic effects

In addition to the choice of templates, which is treated separately, the measurement suffers from systematic effects due to limited knowledge of backgrounds, charge misidentification, choice of PDF sets, uncertainties on the lepton energy scale and resolution, and uncertainties on the recoil system energy scale and resolution. The uncertainties on helicity fractions have been estimated using MC@NLO and are reported in Table 7, in absolute terms.

The effect of reweighting simulated events to restore a p_T^W distribution closer to that observed [38] was also assessed.

8.1 Backgrounds

The electroweak and $t\bar{t}$ backgrounds have been studied previously and found to be well modelled by Monte Carlo simulations [33, 41–43]. As these backgrounds are subtracted

Table 5 Values of the χ^2 from the fit of data with MC@NLO and POWHEG helicity templates (see Figs. 7 and 8 for MC@NLO). The number of degrees of freedom in the fits is 17

χ^2 between data and	$35 < p_T^W < 50$ GeV				$p_T^W > 50$ GeV			
	μ^+	μ^-	e^+	e^-	μ^+	μ^-	e^+	e^-
MC@NLO templates	13.5	23.1	7.6	25.3	29.3	21.1	24.8	16.9
POWHEG templates	11.1	20.7	8.2	20.8	30.1	26.6	20.9	13.1

Table 6 Summary of raw data results for helicity fractions (as percentages) for $35 < p_T^W < 50$ GeV and $p_T^W > 50$ GeV obtained with MC@NLO or with POWHEG template fits (see Figs. 7 and 8 for MC@NLO). The errors represent the statistical uncertainties only

		μ^+	μ^-	e^+	e^-
		$35 < p_T^W < 50$ GeV			
Data with MC@NLO	f_0 (%)	26.6 ± 5.1	10.9 ± 5.6	23.2 ± 5.7	9.9 ± 10.2
	$f_L - f_R$ (%)	20.6 ± 3.9	27.1 ± 4.3	17.9 ± 4.2	33.0 ± 4.0
Data with POWHEG	f_0 (%)	42.8 ± 5.1	35.1 ± 5.7	36.9 ± 9.1	26.5 ± 6.1
	$f_L - f_R$ (%)	25.6 ± 3.9	21.8 ± 4.3	21.3 ± 5.3	25.1 ± 4.3
		$p_T^W > 50$ GeV			
Data with MC@NLO	f_0 (%)	8.3 ± 5.0	-0.0 ± 7.3	9.7 ± 5.7	20.0 ± 5.6
	$f_L - f_R$ (%)	27.5 ± 3.3	29.9 ± 3.4	29.3 ± 3.5	19.7 ± 3.9
Data with POWHEG	f_0 (%)	15.3 ± 4.4	13.0 ± 5.0	19.6 ± 5.7	26.6 ± 6.9
	$f_L - f_R$ (%)	27.7 ± 3.2	19.9 ± 3.6	29.5 ± 3.6	13.3 ± 4.2

Fig. 7 Results of the fits to $\cos\theta_{2D}$ distributions using helicity templates (built from MC@NLO), for $W \to \mu\nu$ (*top*) and $W \to e\nu$ (*bottom*) events in data with $35 < p_T^W < 50$ GeV, after background subtraction. Each template distribution is represented: left-handed contribution (*dashed line*), longitudinal contribution (*dotted-dashed line*) and right-handed contribution (*dotted line*)

(a) μ^+

(b) μ^-

(c) e^+
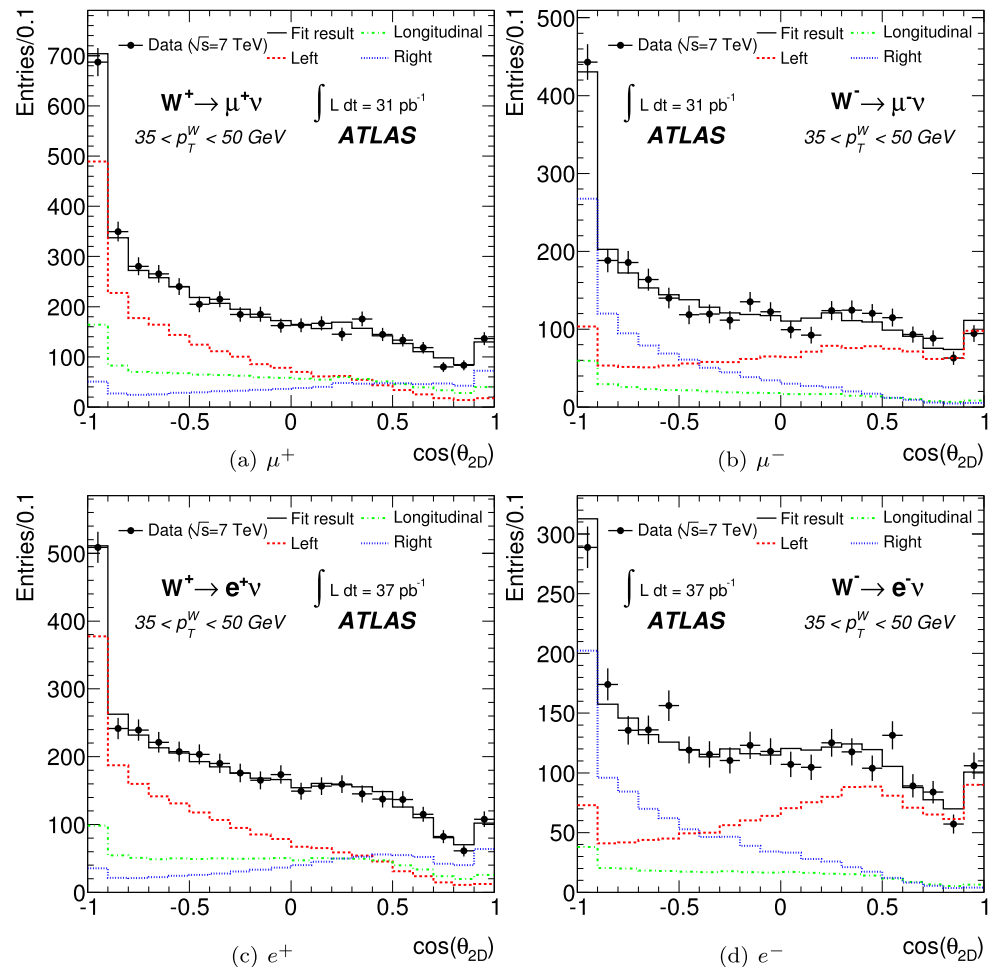
(d) e^-

from data for the final fit, an associated systematic uncertainty has been estimated by changing the global normalisation of the subtracted distributions by ± 6.8 % (± 3.4 % to take into account the uncertainty on the integrated luminosity, ± 5 % for the uncertainty on background cross-sections relative to signal, and ± 3 % for the influence of PDFs on the acceptance [44]).

Furthermore, the amount of jet background was varied inside the uncertainty estimated by the dedicated fit (see Table 2).

8.2 Charge misidentification

Since charge misidentification is well reproduced by simulations [34], the possible associated effect on the results presented here has been measured by comparing helicity fractions extracted from fully simulated events where the charge assignment was taken either from generator-level information or after full reconstruction. The effect on f_0 and $f_L - f_R$ is estimated to be about 0.4 % in the electron case, and is negligible for muons.

8.3 Reweighting of p_T^W distribution

MC@NLO and, to a lesser extent, POWHEG, underestimate the fraction of W events at high p_T^W. In order to investigate the possible consequences of such a bias on this measurement, the MC@NLO Monte Carlo signal sample, weighted event-by-event so as to restore a p_T^W spectrum compatible with data, was fitted using unchanged helicity templates (both POWHEG and MC@NLO templates were used for this test). The effect of the reweighting was found to have a small impact on the fitted values of f_0 (less than 2 %). For $f_L - f_R$ sizeable effects were observed (up to 5 % in the low p_T^W bin). However, they are of opposite sign for the positive and negative lepton charges, and almost perfectly cancel when analysing charge-averaged values (see Table 7).

8.4 PDF sets

Using the PDF reweighting method, the uncertainty associated with PDFs was estimated by keeping the templates unchanged and using MSTW 2008 and HERAPDF 1.0 instead of the CTEQ 6.6 PDFs for the simulation of the signal

Fig. 8 Results of the fits to $\cos\theta_{2D}$ distributions using helicity templates (built from MC@NLO), for $W \to \mu\nu$ (*top*) and $W \to e\nu$ (*bottom*) events in data with $p_T^W > 50$ GeV, after background subtraction. Each template distribution is represented: left-handed contribution (*dashed line*), longitudinal contribution (*dotted-dashed line*) and right-handed contribution (*dotted line*)

(a) μ^+

(b) μ^-

(c) e^+
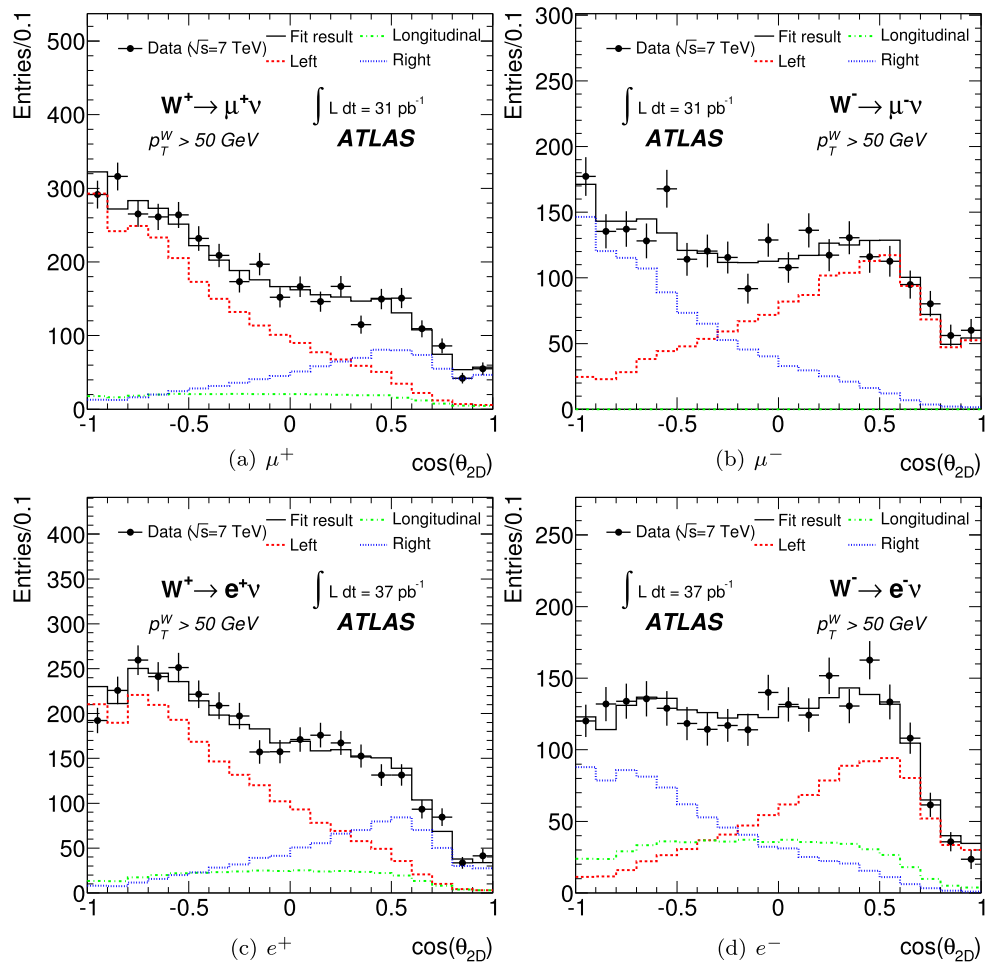
(d) e^-

distributions. The impact on f_0 and $f_L - f_R$ is in the range of 1 % to 2 %.

8.5 Energy scales

While a coherent change of the lepton and recoil energy scales would leave the angles in the transverse plane unchanged, both in the laboratory and in the transverse W rest frame, an effect on $\cos\theta_{2D}$ arises when only one of the two measured objects (lepton, recoil) changes, or if they change by different amounts.

Using simulated events, it has been observed that an increase of the lepton transverse momentum alone gives a positive slope to the $\cos\theta_{2D}$ distribution, which in turn induces an increase of the left-handed fraction in the negative lepton sample, and a decrease of the left-handed fraction in the positive lepton sample. As expected, the reverse happens for an increase of the recoil transverse energy.

The value of $f_L - f_R$ when averaged over the two charges is largely independent of the lepton and recoil energy scales, as can be seen in Table 7.

The same compensation mechanism is however not present for f_0, for which an increase in the recoil energy scale induces an increase of f_0 for both charges.

The lepton energy scale is precisely determined from $Z \to \ell\ell$ decays: using the precisely-known value of the Z boson mass, scale factors have been extracted by η_ℓ regions, which in the muon case depend also on the muon charge [34, 45]. The reconstructed Z boson mass spectrum has also been used to derive smearing corrections to be applied to Monte Carlo electrons and muons in order to reproduce the observed Z mass peak resolution. The resulting uncertainties are about 3 % to 5 % on f_0 and around 2 % on $f_L - f_R$.

For the rather large p_T of the W bosons studied here, the recoil system in general contains one or several jets with $p_T > 20$ GeV, and may also include additional "soft jets" ($7 < p_T < 20$ GeV), and clusters of calorimeter cells not included in the above objects. The uncertainty on the energy scale of these objects (typically 3 % for jets, 10.5 % for soft jets and 13.5 % for isolated clusters) was propagated as described in [46]. This is the largest systematic uncertainty on the helicity fractions measured in this study. In the worst case (muons in the low p_T^W bin), the resulting uncertainty

Table 7 Summary of systematic uncertainties on helicity fractions for $35 < p_T^W < 50$ GeV and $p_T^W > 50$ GeV. The effect of lepton and recoil energy scales, and of p_T^W reweighting, on $f_L - f_R$ is also estimated on the mean between the two charges. The larger errors appear with the $\pm$ ($\mp$) sign if they vary in the same (opposite) direction as the parameter studied, in order to highlight the correlations used in calculating the errors on the means

		$35 < p_T^W < 50$ GeV				$p_T^W > 50$ GeV			
		μ^+	μ^-	e^+	e^-	μ^+	μ^-	e^+	e^-
EW background	δf_0 (%)	0.5	0.6	0.3	0.4	0.6	0.6	0.3	0.5
	$\delta(f_L - f_R)$ (%)	0.2	0.3	0.2	0.2	0.2	0.3	0.2	0.2
Jet background	δf_0 (%)	1.5	1.5	1.5	1.5	2.3	1.3	2	2
	$\delta(f_L - f_R)$ (%)	0.3	0.7	1.5	1.5	1.2	1.3	1.5	1.5
p_T^ℓ scale	δf_0 (%)	$\mp$4.5	$\mp$5.0	$\mp$4.5	$\mp$4.5	$\mp$3.5	$\mp$3.5	$\mp$3.5	$\mp$4.5
	$\delta(f_L - f_R)$ (%)	$\mp$2.5	$\pm$2.0	$\mp$2.5	$\pm$2.0	$\mp$1.5	$\pm$1.5	$\mp$2.0	$\pm$1.5
	$\delta(f_L - f_R)_{\text{mean}}$ (%)	1.1		0.4		0.1		0.4	
Recoil scale	δf_0 (%)	$\pm$12.5	$\pm$16.8	$\pm$12.5	$\pm$13.3	$\pm$8.1	$\pm$10.2	$\pm$9.4	$\pm$11.1
	$\delta(f_L - f_R)$ (%)	$\pm$9.9	$\mp$10.4	$\pm$10.9	$\mp$9.5	$\pm$7.7	$\mp$7.7	$\pm$8.2	$\mp$8.2
	$\delta(f_L - f_R)_{\text{mean}}$ (%)	3.0		2.9		1.2		0.7	
PDF set	δf_0 (%)	2.0	2.0	0.4	0.8	2.0	2.0	0.2	0.8
	$\delta(f_L - f_R)$ (%)	1.5	1.5	0.5	1.5	1.5	1.5	0.4	1.1
Charge misID	δf_0 (%)	–	–	0.2	0.4	–	–	0.2	0.2
	$\delta(f_L - f_R)$ (%)			0.3	0.4			0.2	0.3
p_T^ℓ resolution	δf_0 (%)	0.1	0.1	0.5	0.5	0.1	0.2	0.2	1.2
	$\delta(f_L - f_R)$ (%)	0.1	0.1	0.3	0.3	0.1	0.2	0.2	0.2
p_T^W reweighting	δf_0 (%)	2.5	1.1	0.6	0.9	1.9	1.6	0.5	1.2
	$\delta(f_L - f_R)$ (%)	$\mp$4.9	$\pm$5.2	$\mp$4.2	$\pm$4.0	$\mp$2.7	$\pm$2.9	$\mp$2.6	$\pm$2.3
	$\delta(f_L - f_R)_{\text{mean}}$ (%)	0.2		0.1		0.1		0.2	

on f_0 is 16 %. This uncertainty is largely correlated between the muon and electron channels.

Given the anti-correlation observed between the impacts on positive and negative leptons, the uncertainties from energy scale variations enter with $\pm$ or $\mp$ in Table 7, depending on whether the effect goes in the same direction as an energy increase or in the opposite direction. As already pointed out, in the case of $f_L - f_R$ the effects largely cancel when considering the average between negative and positive charges.

8.6 Choice of the Monte Carlo generator

The results of the template fits to real and fully simulated data are affected by the imperfect correlation between $\cos\theta_{2D}$ and $\cos\theta_{3D}$ and by resolution effects.

In order to compare results directly to theoretical models, the raw results from Sect. 7 are corrected by adding the difference, found using simulations, between the "true" values which would be given by fits to $\cos\theta_{3D}$ distributions obtained at the generator level within acceptance and m_T^W cuts as used here, and the results obtained using fully-simulated $\cos\theta_{2D}$ distributions. In order to be able to average results

from muons and electrons, the electron results are corrected to the same η_ℓ acceptance as for muons (i.e. without the barrel-endcap calorimeters overlap region around 1.5, and with a maximum $|\eta_\ell|$ value of 2.4).

The corrections for results obtained using MC@NLO templates were determined from the difference between:

– results of a fit of MC@NLO (3D) templates to $\cos\theta_{3D}$ distributions of the POWHEG Monte Carlo samples at the generator-level with acceptance and m_T^W cuts;
– results of a fit of MC@NLO (2D) templates to $\cos\theta_{2D}$ distributions of the same POWHEG Monte Carlo samples, after full simulation and with standard plus analysis cuts.

The corrections for results obtained using POWHEG templates were derived in the same way as above, interchanging the roles of MC@NLO and POWHEG.

In a further step, after averaging over the charges for each lepton flavour:

– the corrected data result, for $f_L - f_R$ and f_0, was obtained by averaging the numbers obtained with MC@NLO and with POWHEG templates;

Table 8 Percentage values of $f_L - f_R$ and f_0 averaged over charges, separately for electrons and muons, obtained by averaging results with templates from MC@NLO (see Figs. 7 and 8) and from POWHEG. The first uncertainty is statistical, the second covers the systematic uncertainties from instrumental and analysis effects, and the last one the differences between templates constructed with the two generators

	$35 < p_T^W < 50$ GeV	$p_T^W > 50$ GeV
	$f_L - f_R$ (%)	
Muon average	$21.7 \pm 3.0 \pm 3.6 \pm 2.0$	$25.0 \pm 2.5 \pm 2.3 \pm 2.5$
Electron average	$26.0 \pm 2.8 \pm 3.4 \pm 2.0$	$25.5 \pm 2.6 \pm 2.0 \pm 2.0$
	f_0 (%)	
Muon average	$23.6 \pm 3.8 \pm 12.0 \pm 7.2$	$7.6 \pm 4.8 \pm 9.0 \pm 5.2$
Electron average	$20.1 \pm 6.9 \pm 12.0 \pm 5.0$	$17.7 \pm 4.3 \pm 9.0 \pm 6.0$

Table 9 Corrected values of $f_L - f_R$ and f_0 (as percentages) obtained using SHERPA templates, compared to the standard result (Table 8), for the electron channels averaged over charges. In the SHERPA case the only uncertainty quoted is associated with the two ways of calculating the correction term: applying SHERPA templates either to MC@NLO or to POWHEG simulated data

	$35 < p_T^W < 50$ GeV	$p_T^W > 50$ GeV
	$f_L - f_R$ (%)	
Data (SHERPA)	25.5 ± 2.2	26.6 ± 2
Data (standard)	$26.0 \pm 2.8 \pm 3.4 \pm 2.0$	$25.5 \pm 2.6 \pm 2.0 \pm 2.0$
	f_0 (%)	
Data (SHERPA)	21.0 ± 9.1	15.6 ± 6.1
Data (standard)	$20.1 \pm 6.9 \pm 12.0 \pm 5.0$	$17.7 \pm 4.3 \pm 9.0 \pm 6.0$

– the systematic uncertainty associated with the choice of templates was taken as half the difference between the two numbers, with a minimum value of 2 %.

The corrected results and the associated systematic uncertainties are shown in Table 8 for $f_L - f_R$ and f_0.

The systematic uncertainty associated with the differences between the two sets of templates is large for f_0, for which other systematic effects are also large.

Another correction procedure was tried, using the same Monte Carlo generator for producing the templates and calculating the corrections. The resulting central values of the helicity fractions are very close to those shown in Table 8 (within less than 2 %), but the systematic uncertainties of the corrections are slightly larger (by about 10 % in relative terms).

Finally, a full simulation based on SHERPA 1.2.2 [47], made only for the electron channel, was also used to obtain, similarly as above, first raw results, and then correction terms found by applying SHERPA templates to simulated data produced with both MC@NLO and POWHEG. The corrected measurement obtained in this way are shown in Table 9, together with the "electron average" results from Table 8. In the case of SHERPA, only the uncertainty associated with the choice of template is reported. A very good agreement is observed.

9 Results

The corrected final measurements of $f_L - f_R$, already shown in Table 8, are compared in Table 10 to the values obtained from the MC@NLO and POWHEG samples, at the generator-level with the acceptance and m_T^W cuts, using a template fit to the $\cos\theta_{3D}$ distributions.

In the low p_T bin the data lie in between the MC@NLO and POWHEG predictions, slightly closer to the former. For $p_T^W > 50$ GeV, the data are close to the MC@NLO values,

while POWHEG predicts a somewhat smaller difference between left- and right-handed states than observed in the data.

The same good agreement between data and MC@NLO remains after averaging results over lepton flavours (Table 11). While the complete NNLO cross-section calculation of [7] has not been implemented in a Monte Carlo generator, it can be seen in Fig. 5 and its equivalent (not shown) for BlackHat, that at the particle level, without any cuts, the $f_L - f_R$ values from [7] are on average about 5 % lower (in absolute terms) than the MC@NLO predictions. They are thus quite close to POWHEG and somewhat lower than the data.

The measurements shown in Table 11, where all systematic uncertainties have been combined, are the main result of this study concerning $f_L - f_R$, and the directly related coefficient A_4 (Eq. (5)).

For f_0, and the directly related coefficient A_0 (Eq. (4)), the systematic uncertainties associated with the recoil and lepton energy scales do not cancel between negative and positive charges. In order to reduce the statistical uncertainties, which are also large, and the uncorrelated instrumental and analysis systematic uncertainties, the measurements in each p_T^W bin were averaged over charges and lepton flavours. The uncertainties from the recoil energy scale were taken to be fully correlated among all four measurements. The uncertainty associated with the template model (Table 8) was combined quadratically with the other systematic uncertainties.

A comparison between the corrected experimental results and the predicted values, within the acceptance and m_T^W cuts (Table 11), indicates that:

– in the low p_T^W bin the data are compatible with both MC@NLO and POWHEG predictions, which are mutually consistent;
– in the high p_T^W bin, the data favour f_0 values smaller than the predictions of MC@NLO and POWHEG, which are close to each other.

Table 10 Corrected values, of $f_L - f_R$ (as percentages), averaged over charge, separately for electrons and muons, for the data, MC@NLO and POWHEG, and for $35 < p_T^W < 50$ GeV and $p_T^W > 50$ GeV. For data the first uncertainty is statistical, the second covers the systematic uncertainties from instrumental and analysis effects, and the last one the differences between templates constructed with the two generators. For MC@NLO and POWHEG the uncertainties are only statistical

| | $35 < p_T^W < 50$ GeV | | $p_T^W > 50$ GeV | |
	Muon average	Electron average	Muon average	Electron average
Data	$21.7 \pm 3.0 \pm 3.6 \pm 2.0$	$26.0 \pm 2.8 \pm 3.4 \pm 2.0$	$25.0 \pm 2.5 \pm 2.3 \pm 2.5$	$25.5 \pm 2.6 \pm 2.0 \pm 2.0$
MC@NLO	27.2 ± 0.8	27.1 ± 1.0	26.4 ± 0.8	26.1 ± 0.9
POWHEG	19.9 ± 0.8	19.9 ± 1.0	21.2 ± 0.8	21.2 ± 0.9

Table 11 Corrected values of $f_L - f_R$ and f_0 (as percentages), averaged over charges and lepton flavours, for the data, MC@NLO and POWHEG, and for $35 < p_T^W < 50$ GeV and $p_T^W > 50$ GeV (Fig. 9). For data the first uncertainty is statistical, the second covers all systematic uncertainties. For MC@NLO and POWHEG the uncertainties are only statistical

| | $f_L - f_R$ (%) | | f_0 (%) | |
	$35 < p_T^W < 50$ GeV	$p_T^W > 50$ GeV	$35 < p_T^W < 50$ GeV	$p_T^W > 50$ GeV
Data	$23.8 \pm 2.0 \pm 3.4$	$25.2 \pm 1.7 \pm 3.0$	$21.9 \pm 3.3 \pm 13.4$	$12.7 \pm 3.0 \pm 10.8$
MC@NLO	27.1 ± 0.7	26.2 ± 0.5	17.9 ± 1.2	21.0 ± 1.0
POWHEG	19.9 ± 1.0	21.2 ± 0.8	22.9 ± 1.0	19.4 ± 0.8

Fig. 9 Measured values of f_0 and $f_L - f_R$ after corrections (Table 11), within acceptance cuts, for $35 < p_T^W < 50$ GeV (*left*) and $p_T^W > 50$ GeV (*right*), compared with the predictions of MC@NLO and POWHEG. The ellipses around the data points correspond to one standard deviation
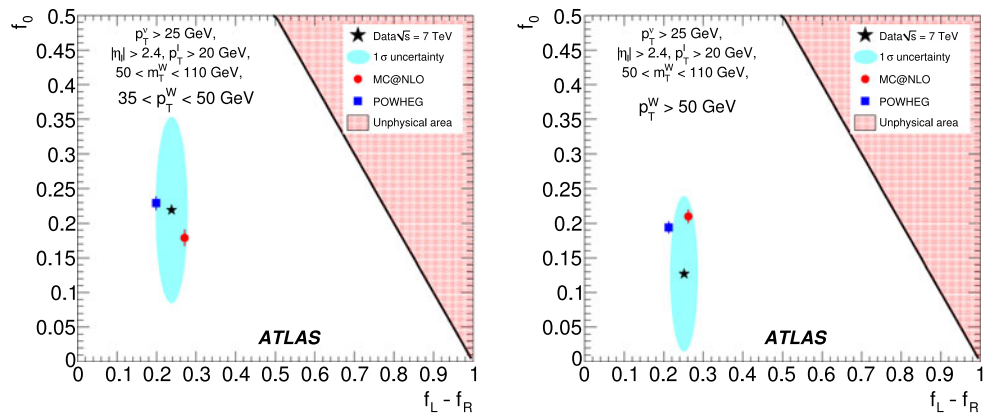
Due to the large uncertainties on the measurements, however, no stringent constraints nor clear inconsistencies can be deduced. The measured values of f_0 and $f_L - f_R$ are plotted in Fig. 9 within the triangular region allowed by the constraint $f_L + f_0 + f_R = 1$, together with the predictions from MC@NLO and POWHEG.

10 Summary and conclusions

The results presented in this paper show that MC@NLO and POWHEG reproduce well the shape of the angular distributions in the transverse plane of charged leptons from high-p_T W boson decays ($p_T^W > 35$ GeV), a regime where the leading-quark effect in quark-antiquark annihilation is subordinate to the dynamics of quark-gluon interactions producing W bosons.

The variable used for the analysis in terms of helicity fractions (respectively f_0, f_L and f_R) is the cosine of the "transverse helicity" angle $\cos\theta_{2D}$. Given that the three helicity fractions are constrained to sum to unity, the independent variables chosen in this study are f_0 and $f_L - f_R$. Their values have been derived by fitting $\cos\theta_{2D}$ distributions with templates representing longitudinal, left- and right-handed W bosons. Two sets of templates were used, obtained from MC@NLO and POWHEG.

The experimental results have been corrected for the difference between the distribution of the measured quantity, the "transverse helicity" angle $\cos\theta_{2D}$, and the distribution of the true helicity angle, $\cos\theta_{3D}$. The correction includes resolution effects, as well as systematic differences between the two sets of templates. Corrected results correspond to

the following acceptance region: $|\eta_\ell| < 2.4$, $p_T^\nu > 25$ GeV, $p_T^\ell > 20$ GeV and $50 < m_T^W < 110$ GeV.

The longitudinal fraction is the most difficult to extract and has rather large systematic uncertainties, especially in the low p_T^W bin, mostly associated with the recoil energy scale and with the choice of Monte Carlo generator. In the low p_T^W bin the data are compatible with both MC@NLO and POWHEG predictions while in the high p_T^W bin, they favour lower values than predicted by either of the simulations, which agree well with each other.

When averaging over charges, $f_L - f_R$ is measured with a small statistical uncertainty and a relatively small systematic uncertainty. The agreement between data and MC@NLO, separately for the four measurements (two lepton flavours and two p_T^W bins) is good. Predictions by POWHEG are somewhat smaller than data, especially in the high p_T^W bin.

References

1. S. Frixione, B.R. Webber, Matching NLO QCD computations and parton shower simulations. J. High Energy Phys. **0206**, 029 (2002)

2. P. Nason, A New method for combining NLO QCD with shower Monte Carlo algorithms. J. High Energy Phys. **0411**, 040 (2004)

3. S. Frixione, P. Nason, C. Oleari, Matching NLO QCD computations with Parton Shower simulations: the POWHEG method. J. High Energy Phys. **0711**, 070 (2007)

4. S. Alioli, P. Nason, C. Oleari, E. Re, A general framework for implementing NLO calculations in shower Monte Carlo programs: the POWHEG BOX. J. High Energy Phys. **06**, 043 (2010)

5. S. Alioli, P. Nason, C. Oleari, E. Re, NLO vector-boson production matched with shower in POWHEG. J. High Energy Phys. **07**, 060 (2008)

6. E. Mirkes, Angular decay distribution of leptons from W bosons at NLO in hadronic collisions. Nucl. Phys. B **387**, 3 (1992)

7. Z. Bern, G. Diana, L. Dixon, F. Febres Cordero, D. Forde et al., Left-Handed W Bosons at the LHC. Phys. Rev. D **84**, 034008 (2011)

8. J. Korner, E. Mirkes, Polarization density matrix of high $q(T)$ gauge bosons in high-energy proton–anti-proton collisions. Nucl. Phys. B, Proc. Suppl. **23**, 9 (1991)

9. J.C. Collins, D.E. Soper, Angular distribution of dileptons in high-energy hadron collisions. Phys. Rev. D **16**, 2219 (1977)

10. C. Lam, W.-K. Tung, A systematic approach to inclusive lepton pair production in hadronic collisions. Phys. Rev. D **18**, 2447 (1978)

11. E. Mirkes, J. Ohnemus, W and Z polarization effects in hadronic collisions. Phys. Rev. D **50**, 5692 (1994)

12. E.L. Berger, J.-W. Qiu, R.A. Rodriguez-Pedraza, Transverse momentum dependence of the angular distribution of the Drell-Yan process. Phys. Rev. D **76**, 074006 (2007)

13. CDF Collaboration, Measurement of the azimuthal angle distribution of leptons from W boson decays as a function of the W transverse momentum in p anti-p collisions at $\sqrt{s} = 1.8$-TeV. Phys. Rev. D **73**, 052002 (2006)

14. H1 Collaboration, Events with isolated leptons and missing transverse momentum and measurement of W production at HERA. Eur. Phys. J. C **64**, 251 (2009)

15. CMS Collaboration, Measurement of the polarization of W bosons with large transverse momenta in $W + \text{Jets}$ events at the LHC. Phys. Rev. Lett. **107**, 021802 (2011)

16. R. Ellis, W. Stirling, B. Webber, QCD and collider physics. Camb. Monogr. Part. Phys. Nucl. Phys. Cosmol. **8**, 1 (1996)

17. ATLAS Collaboration, The ATLAS experiment at the CERN large hadron collider. J. Instrum. **3**, S08003 (2008)

18. ATLAS Collaboration, Performance of the ATLAS trigger system in 2010. Eur. Phys. J. C **72**, 1 (2011)

19. ATLAS Collaboration, Updated luminosity determination in pp collisions at $\sqrt{s} = 7$ TeV using the ATLAS detector. ATLAS-CONF-2011-011. http://cdsweb.cern.ch/record/1334563

20. ATLAS Collaboration, Luminosity determination in pp collisions at $\sqrt{s} = 7$ TeV using the ATLAS detector at the LHC. Eur. Phys. J. C **71**, 1630 (2011)

21. S. Agostinelli et al. (The GEANT4 Collaboration), GEANT4: a simulation toolkit. Nucl. Instrum. Methods A **506**, 250 (2003)

22. ATLAS Collaboration, The ATLAS simulation infrastructure. Eur. Phys. J. C **70**, 823 (2010)

23. G. Corcella, I. Knowles, G. Marchesini, S. Moretti, K. Odagiri et al., HERWIG 6: an event generator for hadron emission reactions with interfering gluons (including supersymmetric processes). J. High Energy Phys. **0101**, 010 (2001)

24. J. Pumplin et al., New generation of parton distributions with uncertainties from global QCD analysis. J. High Energy Phys. **07**, 012 (2002)

25. T. Sjostrand, S. Mrenna, P. Skands, PYTHIA 6.4 physics and manual. J. High Energy Phys. **05**, 026 (2006)

26. A. Tricoli, A.M. Cooper-Sarkar, C. Gwenlan, Uncertainties on W and Z production at the LHC. arXiv:hep-ex/0509002 [hep-ex]

27. A. Martin, W. Stirling, R. Thorne, G. Watt, Parton distributions for the LHC. Eur. Phys. J. C **63**, 189 (2009)

28. H1 and ZEUS Collaboration, Combined measurement and QCD analysis of the inclusive ep scattering cross sections at HERA. J. High Energy Phys. **01**, 109 (2010)

29. P. Golonka, Z. Was, Photos Monte-Carlo: a precision tool for QED corrections in Z and W decays. Eur. Phys. J. C **45**, 97 (2006)

30. N. Davidson, G. Nanava, T. Przedzinski, E. Richter-Was, Z. Was, Universal interface of TAUOLA technical and physics documentation. arXiv:1002.0543 [hep-ph]

31. J. Butterworth, J.R. Forshaw, M. Seymour, Multiparton interactions in photoproduction at HERA. Z. Phys. C **72**, 637 (1996)

32. ATLAS Collaboration, Measurements of underlying-event properties using neutral and charged particles in pp collisions at 900 GeV and 7 TeV with the ATLAS detector at the LHC. Eur. Phys. J. C **71**, 1636 (2011)

33. ATLAS Collaboration, Measurement of the inclusive W± and Z/γ cross sections in the electron and muon decay channels in pp collisions at √s = 7TeV with the ATLAS detector. Phys. Rev. D **85**, 072004 (2012). arXiv:1109.5141 [hep-ex]

34. ATLAS Collaboration, Electron performance measurements with the ATLAS detector using the 2010 LHC proton-proton collision data. Eur. Phys. J. C **72**, 1909 (2012). arXiv:1110.3174 [hep-ex]

35. C. Anastasiou, L. Dixon, K. Melnikov, F. Petriello, High-precision QCD at hadron colliders: electroweak gauge boson rapidity distributions at NNLO. Phys. Rev. D **69**, 094008 (2004)

36. S. Moch, P. Uwer, Heavy-quark pair production at two loops in QCD. Nucl. Phys. Proc. Suppl. **183**, 75–80 (2008)

37. U. Langenfeld, S. Moch, P. Uwer, New results for $t\bar{t}$ production at hadron colliders, in *XVII International Workshop on Deep-Inelastic Scattering and Related Topics*, Madrid, Spain, April 2009. arXiv:0907.2527 [hep-ph]

38. ATLAS Collaboration, Measurement of the transverse momentum distribution of W bosons in pp collisions at √s = 7 TeV with the ATLAS detector. Phys. Rev. D **85**, 012005 (2012)

39. R.J. Barlow, C. Beeston, Fitting using finite Monte Carlo samples. Comput. Phys. Commun. **77**, 219 (1993)

40. R. Brun, F. Rademakers, ROOT—an object oriented data analysis framework, in *Proceedings AIHENP'96 Workshop*, Lausanne, Sep., 1996. Nucl. Inst. Meth., Phys. Res. A, **389**, 81–86 (1997). See also http://root.cern.ch/. The fitter used in this paper is TFractionFitter

41. ATLAS Collaboration, Measurement of the W → τν cross section in pp collisions at √s = 7 TeV with the ATLAS experiment. Phys. Lett. B **706**, 276 (2012)

42. ATLAS Collaboration, Measurement of the Z → ττ cross section with the ATLAS detector. Phys. Rev. D **84**, 112006 (2011)

43. ATLAS Collaboration, Measurement of the top quark pair production cross-section with ATLAS in the single lepton channel. arXiv:1201.1889 [hep-ex]. Phys. Lett. B (submitted)

44. ATLAS Collaboration, Measurement of the W → ℓν and Z/γ* → ℓℓ production cross sections in proton-proton collisions at √s = 7 TeV with the ATLAS detector. J. High Energy Phys. **1012**, 060 (2010)

45. ATLAS Collaboration, Muon momentum resolution in first pass reconstruction of pp collision data recorded by ATLAS in 2010. ATLAS-CONF-2011-046. http://cdsweb.cern.ch/record/1338575

46. ATLAS Collaboration, Performance of missing transverse momentum reconstruction in proton-proton collisions at 7 TeV with ATLAS. Eur. Phys. J. C **72**, 1 (2012)

47. T. Gleisberg, S. Hoeche, F. Krauss, M. Schonherr, S. Schumann et al., Event generation with SHERPA 1.1. J. High Energy Phys. **0902**, 007 (2009)

The ATLAS Collaboration

G. Aad[48], B. Abbott[111], J. Abdallah[11], A.A. Abdelalim[49], A. Abdesselam[118], O. Abdinov[10], B. Abi[112], M. Abolins[88], O.S. AbouZeid[158], H. Abramowicz[153], H. Abreu[115], E. Acerbi[89a,89b], B.S. Acharya[164a,164b], L. Adamczyk[37], D.L. Adams[24], T.N. Addy[56], J. Adelman[175], M. Aderholz[99], S. Adomeit[98], P. Adragna[75], T. Adye[129], S. Aefsky[22], J.A. Aguilar-Saavedra[124b,a], M. Aharrouche[81], S.P. Ahlen[21], F. Ahles[48], A. Ahmad[148], M. Ahsan[40], G. Aielli[133a,133b], T. Akdogan[18a], T.P.A. Åkesson[79], G. Akimoto[155], A.V. Akimov[94], A. Akiyama[67], M.S. Alam[1], M.A. Alam[76], J. Albert[169], S. Albrand[55], M. Aleksa[29], I.N. Aleksandrov[65], F. Alessandria[89a], C. Alexa[25a], G. Alexander[153], G. Alexandre[49], T. Alexopoulos[9], M. Alhroob[20], M. Aliev[15], G. Alimonti[89a], J. Alison[120], M. Aliyev[10], B.M.M. Allbrooke[17], P.P. Allport[73], S.E. Allwood-Spiers[53], J. Almond[82], A. Aloisio[102a,102b], R. Alon[171], A. Alonso[79], B. Alvarez Gonzalez[88], M.G. Alviggi[102a,102b], K. Amako[66], P. Amaral[29], C. Amelung[22], V.V. Ammosov[128], A. Amorim[124a,b], G. Amorós[167], N. Amram[153], C. Anastopoulos[29], L.S. Ancu[16], N. Andari[115], T. Andeen[34], C.F. Anders[20], G. Anders[58a], K.J. Anderson[30], A. Andreazza[89a,89b], V. Andrei[58a], M.-L. Andrieux[55], X.S. Anduaga[70], A. Angerami[34], F. Anghinolfi[29], A. Anisenkov[107], N. Anjos[124a], A. Annovi[47], A. Antonaki[8], M. Antonelli[47], A. Antonov[96], J. Antos[144b], F. Anulli[132a], S. Aoun[83], L. Aperio Bella[4], R. Apolle[118,c], G. Arabidze[88], I. Aracena[143], Y. Arai[66], A.T.H. Arce[44], S. Arfaoui[148], J.-F. Arguin[14], E. Arik[18a,*], M. Arik[18a], A.J. Armbruster[87], O. Arnaez[81], C. Arnault[115], A. Artamonov[95], G. Artoni[132a,132b], D. Arutinov[20], S. Asai[155], R. Asfandiyarov[172], S. Ask[27], B. Åsman[146a,146b], L. Asquith[5], K. Assamagan[24], A. Astbury[169], A. Astvatsatourov[52], B. Aubert[4], E. Auge[115], K. Augsten[127], M. Aurousseau[145a], G. Avolio[163], R. Avramidou[9], D. Axen[168], C. Ay[54], G. Azuelos[93,d], Y. Azuma[155], M.A. Baak[29], G. Baccaglioni[89a], C. Bacci[134a,134b], A.M. Bach[14], H. Bachacou[136], K. Bachas[29], M. Backes[49], M. Backhaus[20], E. Badescu[25a], P. Bagnaia[132a,132b], S. Bahinipati[2], Y. Bai[32a], D.C. Bailey[158], T. Bain[158], J.T. Baines[129], O.K. Baker[175], M.D. Baker[24], S. Baker[77], E. Banas[38], P. Banerjee[93], Sw. Banerjee[172], D. Banfi[29], A. Bangert[150], V. Bansal[169], H.S. Bansil[17], L. Barak[171], S.P. Baranov[94], A. Barashkou[65], A. Barbaro Galtieri[14], T. Barber[48], E.L. Barberio[86], D. Barberis[50a,50b], M. Barbero[20], D.Y. Bardin[65], T. Barillari[99], M. Barisonzi[174], T. Barklow[143], N. Barlow[27], B.M. Barnett[129], R.M. Barnett[14], A. Baroncelli[134a], G. Barone[49], A.J. Barr[118], F. Barreiro[80], J. Barreiro Guimarães da Costa[57], P. Barrillon[115], R. Bartoldus[143],

A.E. Barton[71], V. Bartsch[149], R.L. Bates[53], L. Batkova[144a], J.R. Batley[27], A. Battaglia[16], M. Battistin[29], F. Bauer[136], H.S. Bawa[143,e], S. Beale[98], T. Beau[78], P.H. Beauchemin[161], R. Beccherle[50a], P. Bechtle[20], H.P. Beck[16], S. Becker[98], M. Beckingham[138], K.H. Becks[174], A.J. Beddall[18c], A. Beddall[18c], S. Bedikian[175], V.A. Bednyakov[65], C.P. Bee[83], M. Begel[24], S. Behar Harpaz[152], P.K. Behera[63], M. Beimforde[99], C. Belanger-Champagne[85], P.J. Bell[49], W.H. Bell[49], G. Bella[153], L. Bellagamba[19a], F. Bellina[29], M. Bellomo[29], A. Belloni[57], O. Beloborodova[107,f], K. Belotskiy[96], O. Beltramello[29], S. Ben Ami[152], O. Benary[153], D. Benchekroun[135a], C. Benchouk[83], M. Bendel[81], N. Benekos[165], Y. Benhammou[153], E. Benhar Noccioli[49], J.A. Benitez Garcia[159b], D.P. Benjamin[44], M. Benoit[115], J.R. Bensinger[22], K. Benslama[130], S. Bentvelsen[105], D. Berge[29], E. Bergeaas Kuutmann[41], N. Berger[4], F. Berghaus[169], E. Berglund[105], J. Beringer[14], P. Bernat[77], R. Bernhard[48], C. Bernius[24], T. Berry[76], C. Bertella[83], A. Bertin[19a,19b], F. Bertinelli[29], F. Bertolucci[122a,122b], M.I. Besana[89a,89b], N. Besson[136], S. Bethke[99], W. Bhimji[45], R.M. Bianchi[29], M. Bianco[72a,72b], O. Biebel[98], S.P. Bieniek[77], K. Bierwagen[54], J. Biesiada[14], M. Biglietti[134a], H. Bilokon[47], M. Bindi[19a,19b], S. Binet[115], A. Bingul[18c], C. Bini[132a,132b], C. Biscarat[177], U. Bitenc[48], K.M. Black[21], R.E. Blair[5], J.-B. Blanchard[136], G. Blanchot[29], T. Blazek[144a], C. Blocker[22], J. Blocki[38], A. Blondel[49], W. Blum[81], U. Blumenschein[54], G.J. Bobbink[105], V.B. Bobrovnikov[107], S.S. Bocchetta[79], A. Bocci[44], C.R. Boddy[118], M. Boehler[41], J. Boek[174], N. Boelaert[35], J.A. Bogaerts[29], A. Bogdanchikov[107], A. Bogouch[90,*], C. Bohm[146a], V. Boisvert[76], T. Bold[37], V. Boldea[25a], N.M. Bolnet[136], M. Bona[75], V.G. Bondarenko[96], M. Bondioli[163], M. Boonekamp[136], C.N. Booth[139], S. Bordoni[78], C. Borer[16], A. Borisov[128], G. Borissov[71], I. Borjanovic[12a], M. Borri[82], S. Borroni[87], V. Bortolotto[134a,134b], K. Bos[105], D. Boscherini[19a], M. Bosman[11], H. Boterenbrood[105], D. Botterill[129], J. Bouchami[93], J. Boudreau[123], E.V. Bouhova-Thacker[71], D. Boumediene[33], C. Bourdarios[115], N. Bousson[83], A. Boveia[30], J. Boyd[29], I.R. Boyko[65], N.I. Bozhko[128], I. Bozovic-Jelisavcic[12b], J. Bracinik[17], A. Braem[29], P. Branchini[134a], G.W. Brandenburg[57], A. Brandt[7], G. Brandt[118], O. Brandt[54], U. Bratzler[156], B. Brau[84], J.E. Brau[114], H.M. Braun[174], B. Brelier[158], J. Bremer[29], R. Brenner[166], S. Bressler[171], D. Britton[53], F.M. Brochu[27], I. Brock[20], R. Brock[88], T.J. Brodbeck[71], E. Brodet[153], F. Broggi[89a], C. Bromberg[88], J. Bronner[99], G. Brooijmans[34], W.K. Brooks[31b], G. Brown[82], H. Brown[7], P.A. Bruckman de Renstrom[38], D. Bruncko[144b], R. Bruneliere[48], S. Brunet[61], A. Bruni[19a], G. Bruni[19a], M. Bruschi[19a], T. Buanes[13], Q. Buat[55], F. Bucci[49], J. Buchanan[118], N.J. Buchanan[2], P. Buchholz[141], R.M. Buckingham[118], A.G. Buckley[45], S.I. Buda[25a], I.A. Budagov[65], B. Budick[108], V. Büscher[81], L. Bugge[117], O. Bulekov[96], M. Bunse[42], T. Buran[117], H. Burckhart[29], S. Burdin[73], T. Burgess[13], S. Burke[129], E. Busato[33], P. Bussey[53], C.P. Buszello[166], F. Butin[29], B. Butler[143], J.M. Butler[21], C.M. Buttar[53], J.M. Butterworth[77], W. Buttinger[27], S. Cabrera Urbán[167], D. Caforio[19a,19b], O. Cakir[3a], P. Calafiura[14], G. Calderini[78], P. Calfayan[98], R. Calkins[106], L.P. Caloba[23a], R. Caloi[132a,132b], D. Calvet[33], S. Calvet[33], R. Camacho Toro[33], P. Camarri[133a,133b], M. Cambiaghi[119a,119b], D. Cameron[117], L.M. Caminada[14], S. Campana[29], M. Campanelli[77], V. Canale[102a,102b], F. Canelli[30,g], A. Canepa[159a], J. Cantero[80], L. Capasso[102a,102b], M.D.M. Capeans Garrido[29], I. Caprini[25a], M. Caprini[25a], D. Capriotti[99], M. Capua[36a,36b], R. Caputo[81], C. Caramarcu[24], R. Cardarelli[133a], T. Carli[29], G. Carlino[102a], L. Carminati[89a,89b], B. Caron[85], S. Caron[104], G.D. Carrillo Montoya[172], A.A. Carter[75], J.R. Carter[27], J. Carvalho[124a,h], D. Casadei[108], M.P. Casado[11], M. Cascella[122a,122b], C. Caso[50a,50b,*], A.M. Castaneda Hernandez[172], E. Castaneda-Miranda[172], V. Castillo Gimenez[167], N.F. Castro[124a], G. Cataldi[72a], F. Cataneo[29], A. Catinaccio[29], J.R. Catmore[29], A. Cattai[29], G. Cattani[133a,133b], S. Caughron[88], D. Cauz[164a,164c], P. Cavalleri[78], D. Cavalli[89a], M. Cavalli-Sforza[11], V. Cavasinni[122a,122b], F. Ceradini[134a,134b], A.S. Cerqueira[23b], A. Cerri[29], L. Cerrito[75], F. Cerutti[47], S.A. Cetin[18b], F. Cevenini[102a,102b], A. Chafaq[135a], D. Chakraborty[106], K. Chan[2], B. Chapleau[85], J.D. Chapman[27], J.W. Chapman[87], E. Chareyre[78], D.G. Charlton[17], V. Chavda[82], C.A. Chavez Barajas[29], S. Cheatham[85], S. Chekanov[5], S.V. Chekulaev[159a], G.A. Chelkov[65], M.A. Chelstowska[104], C. Chen[64], H. Chen[24], S. Chen[32c], T. Chen[32c], X. Chen[172], S. Cheng[32a], A. Cheplakov[65], V.F. Chepurnov[65], R. Cherkaoui El Moursli[135e], V. Chernyatin[24], E. Cheu[6], S.L. Cheung[158], L. Chevalier[136], G. Chiefari[102a,102b], L. Chikovani[51a], J.T. Childers[29], A. Chilingarov[71], G. Chiodini[72a], A.S. Chisholm[17], M.V. Chizhov[65], G. Choudalakis[30], S. Chouridou[137], I.A. Christidi[77], A. Christov[48], D. Chromek-Burckhart[29], M.L. Chu[151], J. Chudoba[125], G. Ciapetti[132a,132b], K. Ciba[37], A.K. Ciftci[3a], R. Ciftci[3a], D. Cinca[33], V. Cindro[74], M.D. Ciobotaru[163], C. Ciocca[19a], A. Ciocio[14], M. Cirilli[87], M. Citterio[89a], M. Ciubancan[25a], A. Clark[49], P.J. Clark[45], W. Cleland[123], J.C. Clemens[83], B. Clement[55], C. Clement[146a,146b], R.W. Clifft[129], Y. Coadou[83], M. Cobal[164a,164c], A. Coccaro[172], J. Cochran[64], P. Coe[118], J.G. Cogan[143], J. Coggeshall[165], E. Cogneras[177], J. Colas[4], A.P. Colijn[105], N.J. Collins[17], C. Collins-Tooth[53], J. Collot[55], G. Colon[84], P. Conde Muiño[124a], E. Coniavitis[118], M.C. Conidi[11], M. Consonni[104], V. Consorti[48], S. Constantinescu[25a], C. Conta[119a,119b], F. Conventi[102a,i], J. Cook[29], M. Cooke[14], B.D. Cooper[77], A.M. Cooper-Sarkar[118], K. Copic[14], T. Cornelissen[174], M. Corradi[19a], F. Corriveau[85,j], A. Cortes-Gonzalez[165], G. Cortiana[99], G. Costa[89a], M.J. Costa[167], D. Costanzo[139], T. Costin[30], D. Côté[29], R. Coura Torres[23a], L. Courneyea[169], G. Cowan[76], C. Cowden[27], B.E. Cox[82], K. Cranmer[108], F. Crescioli[122a,122b], M. Cristinziani[20], G. Crosetti[36a,36b], R. Crupi[72a,72b], S. Crépé-Renaudin[55], C.-M. Cuciuc[25a], C. Cuenca Almenar[175], T. Cuhadar Donszelmann[139], M. Curatolo[47], C.J. Curtis[17], C. Cuthbert[150], P. Cwetanski[61], H. Czirr[141], P. Czodrowski[43], Z. Czyczula[175], S. D'Auria[53], M. D'Onofrio[73], A. D'Orazio[132a,132b], P.V.M. Da Silva[23a],

C. Da Via[82], W. Dabrowski[37], T. Dai[87], C. Dallapiccola[84], M. Dam[35], M. Dameri[50a,50b], D.S. Damiani[137], H.O. Danielsson[29], D. Dannheim[99], V. Dao[49], G. Darbo[50a], G.L. Darlea[25b], W. Davey[20], T. Davidek[126], N. Davidson[86], R. Davidson[71], E. Davies[118,c], M. Davies[93], A.R. Davison[77], Y. Davygora[58a], E. Dawe[142], I. Dawson[139], J.W. Dawson[5,*], R.K. Daya-Ishmukhametova[22], K. De[7], R. de Asmundis[102a], S. De Castro[19a,19b], P.E. De Castro Faria Salgado[24], S. De Cecco[78], J. de Graat[98], N. De Groot[104], P. de Jong[105], C. De La Taille[115], H. De la Torre[80], B. De Lotto[164a,164c], L. de Mora[71], L. De Nooij[105], D. De Pedis[132a], A. De Salvo[132a], U. De Sanctis[164a,164c], A. De Santo[149], J.B. De Vivie De Regie[115], S. Dean[77], W.J. Dearnaley[71], R. Debbe[24], C. Debenedetti[45], D.V. Dedovich[65], J. Degenhardt[120], M. Dehchar[118], C. Del Papa[164a,164c], J. Del Peso[80], T. Del Prete[122a,122b], T. Delemontex[55], M. Deliyergiyev[74], A. Dell'Acqua[29], L. Dell'Asta[21], M. Della Pietra[102a,i], D. della Volpe[102a,102b], M. Delmastro[4], N. Delruelle[29], P.A. Delsart[55], C. Deluca[148], S. Demers[175], M. Demichev[65], B. Demirkoz[11,k], J. Deng[163], S.P. Denisov[128], D. Derendarz[38], J.E. Derkaoui[135d], F. Derue[78], P. Dervan[73], K. Desch[20], E. Devetak[148], P.O. Deviveiros[105], A. Dewhurst[129], B. DeWilde[148], S. Dhaliwal[158], R. Dhullipudi[24,l], A. Di Ciaccio[133a,133b], L. Di Ciaccio[4], A. Di Girolamo[29], B. Di Girolamo[29], S. Di Luise[134a,134b], A. Di Mattia[172], B. Di Micco[29], R. Di Nardo[47], A. Di Simone[133a,133b], R. Di Sipio[19a,19b], M.A. Diaz[31a], F. Diblen[18c], E.B. Diehl[87], J. Dietrich[41], T.A. Dietzsch[58a], S. Diglio[86], K. Dindar Yagci[39], J. Dingfelder[20], C. Dionisi[132a,132b], P. Dita[25a], S. Dita[25a], F. Dittus[29], F. Djama[83], T. Djobava[51b], M.A.B. do Vale[23c], A. Do Valle Wemans[124a], T.K.O. Doan[4], M. Dobbs[85], R. Dobinson[29,*], D. Dobos[29], E. Dobson[29,m], J. Dodd[34], C. Doglioni[49], T. Doherty[53], Y. Doi[66,*], J. Dolejsi[126], I. Dolenc[74], Z. Dolezal[126], B.A. Dolgoshein[96,*], T. Dohmae[155], M. Donadelli[23d], M. Donega[120], J. Donini[33], J. Dopke[29], A. Doria[102a], A. Dos Anjos[172], M. Dosil[11], A. Dotti[122a,122b], M.T. Dova[70], J.D. Dowell[17], A.D. Doxiadis[105], A.T. Doyle[53], Z. Drasal[126], J. Drees[174], N. Dressnandt[120], H. Drevermann[29], C. Driouichi[35], M. Dris[9], J. Dubbert[99], S. Dube[14], E. Duchovni[171], G. Duckeck[98], A. Dudarev[29], F. Dudziak[64], M. Dührssen[29], I.P. Duerdoth[82], L. Duflot[115], M.-A. Dufour[85], M. Dunford[29], H. Duran Yildiz[3a], R. Duxfield[139], M. Dwuznik[37], F. Dydak[29], M. Düren[52], W.L. Ebenstein[44], J. Ebke[98], S. Eckweiler[81], K. Edmonds[81], C.A. Edwards[76], N.C. Edwards[53], W. Ehrenfeld[41], T. Ehrich[99], T. Eifert[143], G. Eigen[13], K. Einsweiler[14], E. Eisenhandler[75], T. Ekelof[166], M. El Kacimi[135c], M. Ellert[166], S. Elles[4], F. Ellinghaus[81], K. Ellis[75], N. Ellis[29], J. Elmsheuser[98], M. Elsing[29], D. Emeliyanov[129], R. Engelmann[148], A. Engl[98], B. Epp[62], A. Eppig[87], J. Erdmann[54], A. Ereditato[16], D. Eriksson[146a], J. Ernst[1], M. Ernst[24], J. Ernwein[136], D. Errede[165], S. Errede[165], E. Ertel[81], M. Escalier[115], C. Escobar[123], X. Espinal Curull[11], B. Esposito[47], F. Etienne[83], A.I. Etienvre[136], E. Etzion[153], D. Evangelakou[54], H. Evans[61], L. Fabbri[19a,19b], C. Fabre[29], R.M. Fakhrutdinov[128], S. Falciano[132a], Y. Fang[172], M. Fanti[89a,89b], A. Farbin[7], A. Farilla[134a], J. Farley[148], T. Farooque[158], S.M. Farrington[118], P. Farthouat[29], P. Fassnacht[29], D. Fassouliotis[8], B. Fatholahzadeh[158], A. Favareto[89a,89b], L. Fayard[115], S. Fazio[36a,36b], R. Febbraro[33], P. Federic[144a], O.L. Fedin[121], W. Fedorko[88], M. Fehling-Kaschek[48], L. Feligioni[83], D. Fellmann[5], C. Feng[32d], E.J. Feng[30], A.B. Fenyuk[128], J. Ferencei[144b], J. Ferland[93], W. Fernando[109], S. Ferrag[53], J. Ferrando[53], V. Ferrara[41], A. Ferrari[166], P. Ferrari[105], R. Ferrari[119a], D.E. Ferreira de Lima[53], A. Ferrer[167], M.L. Ferrer[47], D. Ferrere[49], C. Ferretti[87], A. Ferretto Parodi[50a,50b], M. Fiascaris[30], F. Fiedler[81], A. Filipčič[74], A. Filippas[9], F. Filthaut[104], M. Fincke-Keeler[169], M.C.N. Fiolhais[124a,h], L. Fiorini[167], A. Firan[39], G. Fischer[41], P. Fischer[20], M.J. Fisher[109], M. Flechl[48], I. Fleck[141], J. Fleckner[81], P. Fleischmann[173], S. Fleischmann[174], T. Flick[174], A. Floderus[79], L.R. Flores Castillo[172], M.J. Flowerdew[99], M. Fokitis[9], T. Fonseca Martin[16], D.A. Forbush[138], A. Formica[136], A. Forti[82], D. Fortin[159a], J.M. Foster[82], D. Fournier[115], A. Foussat[29], A.J. Fowler[44], K. Fowler[137], H. Fox[71], P. Francavilla[11], S. Franchino[119a,119b], D. Francis[29], T. Frank[171], M. Franklin[57], S. Franz[29], M. Fraternali[119a,119b], S. Fratina[120], S.T. French[27], F. Friedrich[43], R. Froeschl[29], D. Froidevaux[29], J.A. Frost[27], C. Fukunaga[156], E. Fullana Torregrosa[29], J. Fuster[167], C. Gabaldon[29], O. Gabizon[171], T. Gadfort[24], S. Gadomski[49], G. Gagliardi[50a,50b], P. Gagnon[61], C. Galea[98], E.J. Gallas[118], V. Gallo[16], B.J. Gallop[129], P. Gallus[125], K.K. Gan[109], Y.S. Gao[143,e], V.A. Gapienko[128], A. Gaponenko[14], F. Garberson[175], M. Garcia-Sciveres[14], C. García[167], J.E. García Navarro[167], R.W. Gardner[30], N. Garelli[29], H. Garitaonandia[105], V. Garonne[29], J. Garvey[17], C. Gatti[47], G. Gaudio[119a], B. Gaur[141], L. Gauthier[136], I.L. Gavrilenko[94], C. Gay[168], G. Gaycken[20], J.-C. Gayde[29], E.N. Gazis[9], P. Ge[32d], C.N.P. Gee[129], D.A.A. Geerts[105], Ch. Geich-Gimbel[20], K. Gellerstedt[146a,146b], C. Gemme[50a], A. Gemmell[53], M.H. Genest[55], S. Gentile[132a,132b], M. George[54], S. George[76], P. Gerlach[174], A. Gershon[153], C. Geweniger[58a], H. Ghazlane[135b], N. Ghodbane[33], B. Giacobbe[19a], S. Giagu[132a,132b], V. Giakoumopoulou[8], V. Giangiobbe[11], F. Gianotti[29], B. Gibbard[24], A. Gibson[158], S.M. Gibson[29], L.M. Gilbert[118], V. Gilewsky[91], D. Gillberg[28], A.R. Gillman[129], D.M. Gingrich[2,d], J. Ginzburg[153], N. Giokaris[8], M.P. Giordani[164c], R. Giordano[102a,102b], F.M. Giorgi[15], P. Giovannini[99], P.F. Giraud[136], D. Giugni[89a], M. Giunta[93], P. Giusti[19a], B.K. Gjelsten[117], L.K. Gladilin[97], C. Glasman[80], J. Glatzer[48], A. Glazov[41], K.W. Glitza[174], G.L. Glonti[65], J.R. Goddard[75], J. Godfrey[142], J. Godlewski[29], M. Goebel[41], T. Göpfert[43], C. Goeringer[81], C. Gössling[42], T. Göttfert[99], S. Goldfarb[87], T. Golling[175], A. Gomes[124a,b], L.S. Gomez Fajardo[41], R. Gonçalo[76], J. Goncalves Pinto Firmino Da Costa[41], L. Gonella[20], A. Gonidec[29], S. Gonzalez[172], S. González de la Hoz[167], G. Gonzalez Parra[11], M.L. Gonzalez Silva[26], S. Gonzalez-Sevilla[49], J.J. Goodson[148], L. Goossens[29], P.A. Gorbounov[95], H.A. Gordon[24], I. Gorelov[103], G. Gorfine[174], B. Gorini[29], E. Gorini[72a,72b], A. Gorišek[74],

E. Gornicki[38], S.A. Gorokhov[128], V.N. Goryachev[128], B. Gosdzik[41], M. Gosselink[105], M.I. Gostkin[65], I. Gough Eschrich[163], M. Gouighri[135a], D. Goujdami[135c], M.P. Goulette[49], A.G. Goussiou[138], C. Goy[4], S. Gozpinar[22], I. Grabowska-Bold[37], P. Grafström[29], K.-J. Grahn[41], F. Grancagnolo[72a], S. Grancagnolo[15], V. Grassi[148], V. Gratchev[121], N. Grau[34], H.M. Gray[29], J.A. Gray[148], E. Graziani[134a], O.G. Grebenyuk[121], T. Greenshaw[73], Z.D. Greenwood[24,l], K. Gregersen[35], I.M. Gregor[41], P. Grenier[143], J. Griffiths[138], N. Grigalashvili[65], A.A. Grillo[137], S. Grinstein[11], Y.V. Grishkevich[97], J.-F. Grivaz[115], M. Groh[99], E. Gross[171], J. Grosse-Knetter[54], J. Groth-Jensen[171], K. Grybel[141], V.J. Guarino[5], D. Guest[175], C. Guicheney[33], A. Guida[72a,72b], S. Guindon[54], H. Guler[85,n], J. Gunther[125], B. Guo[158], J. Guo[34], A. Gupta[30], Y. Gusakov[65], V.N. Gushchin[128], P. Gutierrez[111], N. Guttman[153], O. Gutzwiller[172], C. Guyot[136], C. Gwenlan[118], C.B. Gwilliam[73], A. Haas[143], S. Haas[29], C. Haber[14], H.K. Hadavand[39], D.R. Hadley[17], P. Haefner[99], F. Hahn[29], S. Haider[29], Z. Hajduk[38], H. Hakobyan[176], D. Hall[118], J. Haller[54], K. Hamacher[174], P. Hamal[113], M. Hamer[54], A. Hamilton[145b,o], S. Hamilton[161], H. Han[32a], L. Han[32b], K. Hanagaki[116], K. Hanawa[160], M. Hance[14], C. Handel[81], P. Hanke[58a], J.R. Hansen[35], J.B. Hansen[35], J.D. Hansen[35], P.H. Hansen[35], P. Hansson[143], K. Hara[160], G.A. Hare[137], T. Harenberg[174], S. Harkusha[90], D. Harper[87], R.D. Harrington[45], O.M. Harris[138], K. Harrison[17], J. Hartert[48], F. Hartjes[105], T. Haruyama[66], A. Harvey[56], S. Hasegawa[101], Y. Hasegawa[140], S. Hassani[136], M. Hatch[29], D. Hauff[99], S. Haug[16], M. Hauschild[29], R. Hauser[88], M. Havranek[20], B.M. Hawes[118], C.M. Hawkes[17], R.J. Hawkings[29], A.D. Hawkins[79], D. Hawkins[163], T. Hayakawa[67], T. Hayashi[160], D. Hayden[76], H.S. Hayward[73], S.J. Haywood[129], E. Hazen[21], M. He[32d], S.J. Head[17], V. Hedberg[79], L. Heelan[7], S. Heim[88], B. Heinemann[14], S. Heisterkamp[35], L. Helary[4], C. Heller[98], M. Heller[29], S. Hellman[146a,146b], D. Hellmich[20], C. Helsens[11], R.C.W. Henderson[71], M. Henke[58a], A. Henrichs[54], A.M. Henriques Correia[29], S. Henrot-Versille[115], F. Henry-Couannier[83], C. Hensel[54], T. Henß[174], C.M. Hernandez[7], Y. Hernández Jiménez[167], R. Herrberg[15], A.D. Hershenhorn[152], G. Herten[48], R. Hertenberger[98], L. Hervas[29], G.G. Hesketh[77], N.P. Hessey[105], E. Higón-Rodriguez[167], D. Hill[5,*], J.C. Hill[27], N. Hill[5], K.H. Hiller[41], S. Hillert[20], S.J. Hillier[17], I. Hinchliffe[14], E. Hines[120], M. Hirose[116], F. Hirsch[42], D. Hirschbuehl[174], J. Hobbs[148], N. Hod[153], M.C. Hodgkinson[139], P. Hodgson[139], A. Hoecker[29], M.R. Hoeferkamp[103], J. Hoffman[39], D. Hoffmann[83], M. Hohlfeld[81], M. Holder[141], S.O. Holmgren[146a], T. Holy[127], J.L. Holzbauer[88], Y. Homma[67], T.M. Hong[120], L. Hooft van Huysduynen[108], T. Horazdovsky[127], C. Horn[143], S. Horner[48], J.-Y. Hostachy[55], S. Hou[151], M.A. Houlden[73], A. Hoummada[135a], J. Howarth[82], D.F. Howell[118], I. Hristova[15], J. Hrivnac[115], I. Hruska[125], T. Hryn'ova[4], P.J. Hsu[81], S.-C. Hsu[14], G.S. Huang[111], Z. Hubacek[127], F. Hubaut[83], F. Huegging[20], A. Huettmann[41], T.B. Huffman[118], E.W. Hughes[34], G. Hughes[71], R.E. Hughes-Jones[82], M. Huhtinen[29], P. Hurst[57], M. Hurwitz[14], U. Husemann[41], N. Huseynov[65,p], J. Huston[88], J. Huth[57], G. Iacobucci[49], G. Iakovidis[9], M. Ibbotson[82], I. Ibragimov[141], R. Ichimiya[67], L. Iconomidou-Fayard[115], J. Idarraga[115], P. Iengo[102a], O. Igonkina[105], Y. Ikegami[66], M. Ikeno[66], Y. Ilchenko[39], D. Iliadis[154], N. Ilic[158], M. Imori[155], T. Ince[20], J. Inigo-Golfin[29], P. Ioannou[8], M. Iodice[134a], V. Ippolito[132a,132b], A. Irles Quiles[167], C. Isaksson[166], A. Ishikawa[67], M. Ishino[68], R. Ishmukhametov[39], C. Issever[118], S. Istin[18a], A.V. Ivashin[128], W. Iwanski[38], H. Iwasaki[66], J.M. Izen[40], V. Izzo[102a], B. Jackson[120], J.N. Jackson[73], P. Jackson[143], M.R. Jaekel[29], V. Jain[61], K. Jakobs[48], S. Jakobsen[35], J. Jakubek[127], D.K. Jana[111], E. Jankowski[158], E. Jansen[77], H. Jansen[29], A. Jantsch[99], M. Janus[20], G. Jarlskog[79], L. Jeanty[57], K. Jelen[37], I. Jen-La Plante[30], P. Jenni[29], A. Jeremie[4], P. Jež[35], S. Jézéquel[4], M.K. Jha[19a], H. Ji[172], W. Ji[81], J. Jia[148], Y. Jiang[32b], M. Jimenez Belenguer[41], G. Jin[32b], S. Jin[32a], O. Jinnouchi[157], M.D. Joergensen[35], D. Joffe[39], L.G. Johansen[13], M. Johansen[146a,146b], K.E. Johansson[146a], P. Johansson[139], S. Johnert[41], K.A. Johns[6], K. Jon-And[146a,146b], G. Jones[118], R.W.L. Jones[71], T.W. Jones[77], T.J. Jones[73], O. Jonsson[29], C. Joram[29], P.M. Jorge[124a], J. Joseph[14], J. Jovicevic[147], T. Jovin[12b], X. Ju[172], C.A. Jung[42], R.M. Jungst[29], V. Juranek[125], P. Jussel[62], A. Juste Rozas[11], V.V. Kabachenko[128], S. Kabana[16], M. Kaci[167], A. Kaczmarska[38], P. Kadlecik[35], M. Kado[115], H. Kagan[109], M. Kagan[57], S. Kaiser[99], E. Kajomovitz[152], S. Kalinin[174], L.V. Kalinovskaya[65], S. Kama[39], N. Kanaya[155], M. Kaneda[29], S. Kaneti[27], T. Kanno[157], V.A. Kantserov[96], J. Kanzaki[66], B. Kaplan[175], A. Kapliy[30], J. Kaplon[29], D. Kar[43], M. Karagounis[20], M. Karagoz[118], M. Karnevskiy[41], K. Karr[5], V. Kartvelishvili[71], A.N. Karyukhin[128], L. Kashif[172], G. Kasieczka[58b], R.D. Kass[109], A. Kastanas[13], M. Kataoka[4], Y. Kataoka[155], E. Katsoufis[9], J. Katzy[41], V. Kaushik[6], K. Kawagoe[67], T. Kawamoto[155], G. Kawamura[81], M.S. Kayl[105], V.A. Kazanin[107], M.Y. Kazarinov[65], R. Keeler[169], R. Kehoe[39], M. Keil[54], G.D. Kekelidze[65], J. Kennedy[98], C.J. Kenney[143], M. Kenyon[53], O. Kepka[125], N. Kerschen[29], B.P. Kerševan[74], S. Kersten[174], K. Kessoku[155], J. Keung[158], F. Khalil-zada[10], H. Khandanyan[165], A. Khanov[112], D. Kharchenko[65], A. Khodinov[96], A.G. Kholodenko[128], A. Khomich[58a], T.J. Khoo[27], G. Khoriauli[20], A. Khoroshilov[174], N. Khovanskiy[65], V. Khovanskiy[95], E. Khramov[65], J. Khubua[51b], H. Kim[146a,146b], M.S. Kim[2], S.H. Kim[160], N. Kimura[170], O. Kind[15], B.T. King[73], M. King[67], R.S.B. King[118], J. Kirk[129], L.E. Kirsch[22], A.E. Kiryunin[99], T. Kishimoto[67], D. Kisielewska[37], T. Kittelmann[123], A.M. Kiver[128], E. Kladiva[144b], J. Klaiber-Lodewigs[42], M. Klein[73], U. Klein[73], K. Kleinknecht[81], M. Klemetti[85], A. Klier[171], P. Klimek[146a,146b], A. Klimentov[24], R. Klingenberg[42], J.A. Klinger[82], E.B. Klinkby[35], T. Klioutchnikova[29], P.F. Klok[104], S. Klous[105], E.-E. Kluge[58a], T. Kluge[73], P. Kluit[105], S. Kluth[99], N.S. Knecht[158], E. Kneringer[62], J. Knobloch[29], E.B.F.G. Knoops[83], A. Knue[54], B.R. Ko[44], T. Kobayashi[155], M. Kobel[43], M. Kocian[143], P. Kodys[126], K. Köneke[29], A.C. König[104], S. Koenig[81], L. Köpke[81], F. Koetsveld[104], P. Koevesarki[20], T. Koffas[28], E. Koffeman[105], L.A. Kogan[118], F. Kohn[54], Z. Kohout[127], T. Kohriki[66], T. Koi[143], T. Kokott[20],

G.M. Kolachev[107], H. Kolanoski[15], V. Kolesnikov[65], I. Koletsou[89a], J. Koll[88], M. Kollefrath[48], S.D. Kolya[82], A.A. Komar[94], Y. Komori[155], T. Kondo[66], T. Kono[41,q], A.I. Kononov[48], R. Konoplich[108,r], N. Konstantinidis[77], A. Kootz[174], S. Koperny[37], K. Korcyl[38], K. Kordas[154], V. Koreshev[128], A. Korn[118], A. Korol[107], I. Korolkov[11], E.V. Korolkova[139], V.A. Korotkov[128], O. Kortner[99], S. Kortner[99], V.V. Kostyukhin[20], M.J. Kotamäki[29], S. Kotov[99], V.M. Kotov[65], A. Kotwal[44], C. Kourkoumelis[8], V. Kouskoura[154], A. Koutsman[159a], R. Kowalewski[169], T.Z. Kowalski[37], W. Kozanecki[136], A.S. Kozhin[128], V. Kral[127], V.A. Kramarenko[97], G. Kramberger[74], M.W. Krasny[78], A. Krasznahorkay[108], J. Kraus[88], J.K. Kraus[20], A. Kreisel[153], F. Krejci[127], J. Kretzschmar[73], N. Krieger[54], P. Krieger[158], K. Kroeninger[54], H. Kroha[99], J. Kroll[120], J. Kroseberg[20], J. Krstic[12a], U. Kruchonak[65], H. Krüger[20], T. Kruker[16], N. Krumnack[64], Z.V. Krumshteyn[65], A. Kruth[20], T. Kubota[86], S. Kuday[3a], S. Kuehn[48], A. Kugel[58c], T. Kuhl[41], D. Kuhn[62], V. Kukhtin[65], Y. Kulchitsky[90], S. Kuleshov[31b], C. Kummer[98], M. Kuna[78], N. Kundu[118], J. Kunkle[120], A. Kupco[125], H. Kurashige[67], M. Kurata[160], Y.A. Kurochkin[90], V. Kus[125], E.S. Kuwertz[147], M. Kuze[157], J. Kvita[142], R. Kwee[15], A. La Rosa[49], L. La Rotonda[36a,36b], L. Labarga[80], J. Labbe[4], S. Lablak[135a], C. Lacasta[167], F. Lacava[132a,132b], H. Lacker[15], D. Lacour[78], V.R. Lacuesta[167], E. Ladygin[65], R. Lafaye[4], B. Laforge[78], T. Lagouri[80], S. Lai[48], E. Laisne[55], M. Lamanna[29], C.L. Lampen[6], W. Lampl[6], E. Lancon[136], U. Landgraf[48], M.P.J. Landon[75], J.L. Lane[82], C. Lange[41], A.J. Lankford[163], F. Lanni[24], K. Lantzsch[174], S. Laplace[78], C. Lapoire[20], J.F. Laporte[136], T. Lari[89a], A.V. Larionov[128], A. Larner[118], C. Lasseur[29], M. Lassnig[29], P. Laurelli[47], V. Lavorini[36a,36b], W. Lavrijsen[14], P. Laycock[73], A.B. Lazarev[65], O. Le Dortz[78], E. Le Guirriec[83], C. Le Maner[158], E. Le Menedeu[9], C. Lebel[93], T. LeCompte[5], F. Ledroit-Guillon[55], H. Lee[105], J.S.H. Lee[116], S.C. Lee[151], L. Lee[175], M. Lefebvre[169], M. Legendre[136], A. Leger[49], B.C. LeGeyt[120], F. Legger[98], C. Leggett[14], M. Lehmacher[20], G. Lehmann Miotto[29], X. Lei[6], M.A.L. Leite[23d], R. Leitner[126], D. Lellouch[171], M. Leltchouk[34], B. Lemmer[54], V. Lendermann[58a], K.J.C. Leney[145b], T. Lenz[105], G. Lenzen[174], B. Lenzi[29], K. Leonhardt[43], S. Leontsinis[9], C. Leroy[93], J.-R. Lessard[169], J. Lesser[146a], C.G. Lester[27], A. Leung Fook Cheong[172], J. Levêque[4], D. Levin[87], L.J. Levinson[171], M.S. Levitski[128], A. Lewis[118], G.H. Lewis[108], A.M. Leyko[20], M. Leyton[15], B. Li[83], H. Li[172,s], S. Li[32b,t], X. Li[87], Z. Liang[118,u], H. Liao[33], B. Liberti[133a], P. Lichard[29], M. Lichtnecker[98], K. Lie[165], W. Liebig[13], R. Lifshitz[152], C. Limbach[20], A. Limosani[86], M. Limper[63], S.C. Lin[151,v], F. Linde[105], J.T. Linnemann[88], E. Lipeles[120], L. Lipinsky[125], A. Lipniacka[13], T.M. Liss[165], D. Lissauer[24], A. Lister[49], A.M. Litke[137], C. Liu[28], D. Liu[151], H. Liu[87], J.B. Liu[87], M. Liu[32b], Y. Liu[32b], M. Livan[119a,119b], S.S.A. Livermore[118], A. Lleres[55], J. Llorente Merino[80], S.L. Lloyd[75], E. Lobodzinska[41], P. Loch[6], W.S. Lockman[137], T. Loddenkoetter[20], F.K. Loebinger[82], A. Loginov[175], C.W. Loh[168], T. Lohse[15], K. Lohwasser[48], M. Lokajicek[125], J. Loken[118], V.P. Lombardo[4], R.E. Long[71], L. Lopes[124a], D. Lopez Mateos[57], J. Lorenz[98], N. Lorenzo Martinez[115], M. Losada[162], P. Loscutoff[14], F. Lo Sterzo[132a,132b], M.J. Losty[159a], X. Lou[40], A. Lounis[115], K.F. Loureiro[162], J. Love[21], P.A. Love[71], A.J. Lowe[143,e], F. Lu[32a], H.J. Lubatti[138], C. Luci[132a,132b], A. Lucotte[55], A. Ludwig[43], D. Ludwig[41], I. Ludwig[48], J. Ludwig[48], F. Luehring[61], G. Luijckx[105], D. Lumb[48], L. Luminari[132a], E. Lund[117], B. Lund-Jensen[147], B. Lundberg[79], J. Lundberg[146a,146b], J. Lundquist[35], M. Lungwitz[81], G. Lutz[99], D. Lynn[24], J. Lys[14], E. Lytken[79], H. Ma[24], L.L. Ma[172], J.A. Macana Goia[93], G. Maccarrone[47], A. Macchiolo[99], B. Maček[74], J. Machado Miguens[124a], R. Mackeprang[35], R.J. Madaras[14], W.F. Mader[43], R. Maenner[58c], T. Maeno[24], P. Mättig[174], S. Mättig[41], L. Magnoni[29], E. Magradze[54], Y. Mahalalel[153], K. Mahboubi[48], G. Mahout[17], C. Maiani[132a,132b], C. Maidantchik[23a], A. Maio[124a,b], S. Majewski[24], Y. Makida[66], N. Makovec[115], P. Mal[136], B. Malaescu[29], Pa. Malecki[38], P. Malecki[38], V.P. Maleev[121], F. Malek[55], U. Mallik[63], D. Malon[5], C. Malone[143], S. Maltezos[9], V. Malyshev[107], S. Malyukov[29], R. Mameghani[98], J. Mamuzic[12b], A. Manabe[66], L. Mandelli[89a], I. Mandić[74], R. Mandrysch[15], J. Maneira[124a], P.S. Mangeard[88], L. Manhaes de Andrade Filho[23a], I.D. Manjavidze[65], A. Mann[54], P.M. Manning[137], A. Manousakis-Katsikakis[8], B. Mansoulie[136], A. Manz[99], A. Mapelli[29], L. Mapelli[29], L. March[80], J.F. Marchand[28], F. Marchese[133a,133b], G. Marchiori[78], M. Marcisovsky[125], C.P. Marino[169], F. Marroquim[23a], R. Marshall[82], Z. Marshall[29], F.K. Martens[158], S. Marti-Garcia[167], A.J. Martin[175], B. Martin[29], B. Martin[88], F.F. Martin[120], J.P. Martin[93], Ph. Martin[55], T.A. Martin[17], V.J. Martin[45], B. Martin dit Latour[49], S. Martin-Haugh[149], M. Martinez[11], V. Martinez Outschoorn[57], A.C. Martyniuk[169], M. Marx[82], F. Marzano[132a], A. Marzin[111], L. Masetti[81], T. Mashimo[155], R. Mashinistov[94], J. Masik[82], A.L. Maslennikov[107], I. Massa[19a,19b], G. Massaro[105], N. Massol[4], P. Mastrandrea[132a,132b], A. Mastroberardino[36a,36b], T. Masubuchi[155], P. Matricon[115], H. Matsumoto[155], H. Matsunaga[155], T. Matsushita[67], C. Mattravers[118,c], J.M. Maugain[29], J. Maurer[83], S.J. Maxfield[73], D.A. Maximov[107,f], E.N. May[5], A. Mayne[139], R. Mazini[151], M. Mazur[20], M. Mazzanti[89a], S.P. Mc Kee[87], A. McCarn[165], R.L. McCarthy[148], T.G. McCarthy[28], N.A. McCubbin[129], K.W. McFarlane[56], J.A. Mcfayden[139], H. McGlone[53], G. Mchedlidze[51b], R.A. McLaren[29], T. Mclaughlan[17], S.J. McMahon[129], R.A. McPherson[169,j], A. Meade[84], J. Mechnich[105], M. Mechtel[174], M. Medinnis[41], R. Meera-Lebbai[111], T. Meguro[116], R. Mehdiyev[93], S. Mehlhase[35], A. Mehta[73], K. Meier[58a], B. Meirose[79], C. Melachrinos[30], B.R. Mellado Garcia[172], L. Mendoza Navas[162], Z. Meng[151,s], A. Mengarelli[19a,19b], S. Menke[99], C. Menot[29], E. Meoni[11], K.M. Mercurio[57], P. Mermod[49], L. Merola[102a,102b], C. Meroni[89a], F.S. Merritt[30], H. Merritt[109], A. Messina[29], J. Metcalfe[103], A.S. Mete[64], C. Meyer[81], C. Meyer[30], J.-P. Meyer[136], J. Meyer[173], J. Meyer[54], T.C. Meyer[29], W.T. Meyer[64], J. Miao[32d], S. Michal[29],

L. Micu[25a], R.P. Middleton[129], S. Migas[73], L. Mijović[41], G. Mikenberg[171], M. Mikestikova[125], M. Mikuž[74], D.W. Miller[30], R.J. Miller[88], W.J. Mills[168], C. Mills[57], A. Milov[171], D.A. Milstead[146a,146b], D. Milstein[171], A.A. Minaenko[128], M. Miñano Moya[167], I.A. Minashvili[65], A.I. Mincer[108], B. Mindur[37], M. Mineev[65], Y. Ming[172], L.M. Mir[11], G. Mirabelli[132a], L. Miralles Verge[11], A. Misiejuk[76], J. Mitrevski[137], G.Y. Mitrofanov[128], V.A. Mitsou[167], S. Mitsui[66], P.S. Miyagawa[139], K. Miyazaki[67], J.U. Mjörnmark[79], T. Moa[146a,146b], P. Mockett[138], S. Moed[57], V. Moeller[27], K. Mönig[41], N. Möser[20], S. Mohapatra[148], W. Mohr[48], S. Mohrdieck-Möck[99], A.M. Moisseev[128,*], R. Moles-Valls[167], J. Molina-Perez[29], J. Monk[77], E. Monnier[83], S. Montesano[89a,89b], F. Monticelli[70], S. Monzani[19a,19b], R.W. Moore[2], G.F. Moorhead[86], C. Mora Herrera[49], A. Moraes[53], N. Morange[136], J. Morel[54], G. Morello[36a,36b], D. Moreno[81], M. Moreno Llácer[167], P. Morettini[50a], M. Morgenstern[43], M. Morii[57], J. Morin[75], A.K. Morley[29], G. Mornacchi[29], S.V. Morozov[96], J.D. Morris[75], L. Morvaj[101], H.G. Moser[99], M. Mosidze[51b], J. Moss[109], R. Mount[143], E. Mountricha[9,w], S.V. Mouraviev[94], E.J.W. Moyse[84], M. Mudrinic[12b], F. Mueller[58a], J. Mueller[123], K. Mueller[20], T.A. Müller[98], T. Mueller[81], D. Muenstermann[29], A. Muir[168], Y. Munwes[153], W.J. Murray[129], I. Mussche[105], E. Musto[102a,102b], A.G. Myagkov[128], M. Myska[125], J. Nadal[11], K. Nagai[160], K. Nagano[66], A. Nagarkar[109], Y. Nagasaka[60], M. Nagel[99], A.M. Nairz[29], Y. Nakahama[29], K. Nakamura[155], T. Nakamura[155], I. Nakano[110], G. Nanava[20], A. Napier[161], R. Narayan[58b], M. Nash[77,c], N.R. Nation[21], T. Nattermann[20], T. Naumann[41], G. Navarro[162], H.A. Neal[87], E. Nebot[80], P.Yu. Nechaeva[94], T.J. Neep[82], A. Negri[119a,119b], G. Negri[29], S. Nektarijevic[49], A. Nelson[163], S. Nelson[143], T.K. Nelson[143], S. Nemecek[125], P. Nemethy[108], A.A. Nepomuceno[23a], M. Nessi[29,x], M.S. Neubauer[165], A. Neusiedl[81], R.M. Neves[108], P. Nevski[24], P.R. Newman[17], V. Nguyen Thi Hong[136], R.B. Nickerson[118], R. Nicolaidou[136], L. Nicolas[139], B. Nicquevert[29], F. Niedercorn[115], J. Nielsen[137], T. Niinikoski[29], N. Nikiforou[34], A. Nikiforov[15], V. Nikolaenko[128], K. Nikolaev[65], I. Nikolic-Audit[78], K. Nikolics[49], K. Nikolopoulos[24], H. Nilsen[48], P. Nilsson[7], Y. Ninomiya[155], A. Nisati[132a], T. Nishiyama[67], R. Nisius[99], L. Nodulman[5], M. Nomachi[116], I. Nomidis[154], M. Nordberg[29], B. Nordkvist[146a,146b], P.R. Norton[129], J. Novakova[126], M. Nozaki[66], L. Nozka[113], I.M. Nugent[159a], A.-E. Nuncio-Quiroz[20], G. Nunes Hanninger[86], T. Nunnemann[98], E. Nurse[77], B.J. O'Brien[45], S.W. O'Neale[17,*], D.C. O'Neil[142], V. O'Shea[53], L.B. Oakes[98], F.G. Oakham[28,d], H. Oberlack[99], J. Ocariz[78], A. Ochi[67], S. Oda[155], S. Odaka[66], J. Odier[83], H. Ogren[61], A. Oh[82], S.H. Oh[44], C.C. Ohm[146a,146b], T. Ohshima[101], H. Ohshita[140], T. Ohsugi[59], S. Okada[67], H. Okawa[163], Y. Okumura[101], T. Okuyama[155], A. Olariu[25a], M. Olcese[50a], A.G. Olchevski[65], S.A. Olivares Pino[31a], M. Oliveira[124a,h], D. Oliveira Damazio[24], E. Oliver Garcia[167], D. Olivito[120], A. Olszewski[38], J. Olszowska[38], C. Omachi[67], A. Onofre[124a,y], P.U.E. Onyisi[30], C.J. Oram[159a], M.J. Oreglia[30], Y. Oren[153], D. Orestano[134a,134b], I. Orlov[107], C. Oropeza Barrera[53], R.S. Orr[158], B. Osculati[50a,50b], R. Ospanov[120], C. Osuna[11], G. Otero y Garzon[26], J.P. Ottersbach[105], M. Ouchrif[135d], E.A. Ouellette[169], F. Ould-Saada[117], A. Ouraou[136], Q. Ouyang[32a], A. Ovcharova[14], M. Owen[82], S. Owen[139], V.E. Ozcan[18a], N. Ozturk[7], A. Pacheco Pages[11], C. Padilla Aranda[11], S. Pagan Griso[14], E. Paganis[139], F. Paige[24], P. Pais[84], K. Pajchel[117], G. Palacino[159b], C.P. Paleari[6], S. Palestini[29], D. Pallin[33], A. Palma[124a], J.D. Palmer[17], Y.B. Pan[172], E. Panagiotopoulou[9], B. Panes[31a], N. Panikashvili[87], S. Panitkin[24], D. Pantea[25a], M. Panuskova[125], V. Paolone[123], A. Papadelis[146a], Th.D. Papadopoulou[9], A. Paramonov[5], D. Paredes Hernandez[33], W. Park[24,z], M.A. Parker[27], F. Parodi[50a,50b], J.A. Parsons[34], U. Parzefall[48], E. Pasqualucci[132a], S. Passaggio[50a], A. Passeri[134a], F. Pastore[134a,134b], Fr. Pastore[76], G. Pásztor[49,aa], S. Pataraia[174], N. Patel[150], J.R. Pater[82], S. Patricelli[102a,102b], T. Pauly[29], M. Pecsy[144a], M.I. Pedraza Morales[172], S.V. Peleganchuk[107], H. Peng[32b], R. Pengo[29], B. Penning[30], A. Penson[34], J. Penwell[61], M. Perantoni[23a], K. Perez[34,ab], T. Perez Cavalcanti[41], E. Perez Codina[11], M.T. Pérez García-Estañ[167], V. Perez Reale[34], L. Perini[89a,89b], H. Pernegger[29], R. Perrino[72a], P. Perrodo[4], S. Persembe[3a], A. Perus[115], V.D. Peshekhonov[65], K. Peters[29], B.A. Petersen[29], J. Petersen[29], T.C. Petersen[35], E. Petit[4], A. Petridis[154], C. Petridou[154], E. Petrolo[132a], F. Petrucci[134a,134b], D. Petschull[41], M. Petteni[142], R. Pezoa[31b], A. Phan[86], P.W. Phillips[129], G. Piacquadio[29], A. Picazio[49], E. Piccaro[75], M. Piccinini[19a,19b], S.M. Piec[41], R. Piegaia[26], D.T. Pignotti[109], J.E. Pilcher[30], A.D. Pilkington[82], J. Pina[124a,b], M. Pinamonti[164a,164c], A. Pinder[118], J.L. Pinfold[2], J. Ping[32c], B. Pinto[124a], O. Pirotte[29], C. Pizio[89a,89b], M. Plamondon[169], M.-A. Pleier[24], A.V. Pleskach[128], A. Poblaguev[24], S. Poddar[58a], F. Podlyski[33], L. Poggioli[115], T. Poghosyan[20], M. Pohl[49], F. Polci[55], G. Polesello[119a], A. Policicchio[36a,36b], A. Polini[19a], J. Poll[75], V. Polychronakos[24], D.M. Pomarede[136], D. Pomeroy[22], K. Pommès[29], L. Pontecorvo[132a], B.G. Pope[88], G.A. Popeneciu[25a], D.S. Popovic[12a], A. Poppleton[29], X. Portell Bueso[29], C. Posch[21], G.E. Pospelov[99], S. Pospisil[127], I.N. Potrap[99], C.J. Potter[149], C.T. Potter[114], G. Poulard[29], J. Poveda[172], V. Pozdnyakov[65], R. Prabhu[77], P. Pralavorio[83], A. Pranko[14], S. Prasad[29], R. Pravahan[7], S. Prell[64], K. Pretzl[16], L. Pribyl[29], D. Price[61], J. Price[73], L.E. Price[5], M.J. Price[29], D. Prieur[123], M. Primavera[72a], K. Prokofiev[108], F. Prokoshin[31b], S. Protopopescu[24], J. Proudfoot[5], X. Prudent[43], M. Przybycien[37], H. Przysiezniak[4], S. Psoroulas[20], E. Ptacek[114], E. Pueschel[84], J. Purdham[87], M. Purohit[24,z], P. Puzo[115], Y. Pylypchenko[63], J. Qian[87], Z. Qian[83], Z. Qin[41], A. Quadt[54], D.R. Quarrie[14], W.B. Quayle[172], F. Quinonez[31a], M. Raas[104], V. Radescu[58b], B. Radics[20], P. Radloff[114], T. Rador[18a], F. Ragusa[89a,89b], G. Rahal[177], A.M. Rahimi[109], D. Rahm[24], S. Rajagopalan[24], M. Rammensee[48], M. Rammes[141], A.S. Randle-Conde[39], K. Randrianarivony[28], P.N. Ratoff[71], F. Rauscher[98], T.C. Rave[48], M. Raymond[29], A.L. Read[117], D.M. Rebuzzi[119a,119b], A. Redelbach[173], G. Redlinger[24], R. Reece[120], K. Reeves[40], A. Reichold[105], E. Reinherz-Aronis[153], A. Reinsch[114], I. Reisinger[42],

C. Rembser[29], Z.L. Ren[151], A. Renaud[115], M. Rescigno[132a], S. Resconi[89a], B. Resende[136], P. Reznicek[98], R. Rezvani[158], A. Richards[77], R. Richter[99], E. Richter-Was[4,ac], M. Ridel[78], M. Rijpstra[105], M. Rijssenbeek[148], A. Rimoldi[119a,119b], L. Rinaldi[19a], R.R. Rios[39], I. Riu[11], G. Rivoltella[89a,89b], F. Rizatdinova[112], E. Rizvi[75], S.H. Robertson[85,j], A. Robichaud-Veronneau[118], D. Robinson[27], J.E.M. Robinson[77], A. Robson[53], J.G. Rocha de Lima[106], C. Roda[122a,122b], D. Roda Dos Santos[29], D. Rodriguez[162], A. Roe[54], S. Roe[29], O. Røhne[117], V. Rojo[1], S. Rolli[161], A. Romaniouk[96], M. Romano[19a,19b], V.M. Romanov[65], G. Romeo[26], E. Romero Adam[167], L. Roos[78], E. Ros[167], S. Rosati[132a], K. Rosbach[49], A. Rose[149], M. Rose[76], G.A. Rosenbaum[158], E.I. Rosenberg[64], P.L. Rosendahl[13], O. Rosenthal[141], L. Rosselet[49], V. Rossetti[11], E. Rossi[132a,132b], L.P. Rossi[50a], M. Rotaru[25a], I. Roth[171], J. Rothberg[138], D. Rousseau[115], C.R. Royon[136], A. Rozanov[83], Y. Rozen[152], X. Ruan[32a,ad], I. Rubinskiy[41], B. Ruckert[98], N. Ruckstuhl[105], V.I. Rud[97], C. Rudolph[43], G. Rudolph[62], F. Rühr[6], F. Ruggieri[134a,134b], A. Ruiz-Martinez[64], V. Rumiantsev[91,*], L. Rumyantsev[65], K. Runge[48], Z. Rurikova[48], N.A. Rusakovich[65], J.P. Rutherfoord[6], C. Ruwiedel[14], P. Ruzicka[125], Y.F. Ryabov[121], V. Ryadovikov[128], P. Ryan[88], M. Rybar[126], G. Rybkin[115], N.C. Ryder[118], S. Rzaeva[10], A.F. Saavedra[150], I. Sadeh[153], H.F-W. Sadrozinski[137], R. Sadykov[65], F. Safai Tehrani[132a], H. Sakamoto[155], G. Salamanna[75], A. Salamon[133a], M. Saleem[111], D. Salihagic[99], A. Salnikov[143], J. Salt[167], B.M. Salvachua Ferrando[5], D. Salvatore[36a,36b], F. Salvatore[149], A. Salvucci[104], A. Salzburger[29], D. Sampsonidis[154], B.H. Samset[117], A. Sanchez[102a,102b], V. Sanchez Martinez[167], H. Sandaker[13], H.G. Sander[81], M.P. Sanders[98], M. Sandhoff[174], T. Sandoval[27], C. Sandoval[162], R. Sandstroem[99], S. Sandvoss[174], D.P.C. Sankey[129], A. Sansoni[47], C. Santamarina Rios[85], C. Santoni[33], R. Santonico[133a,133b], H. Santos[124a], J.G. Saraiva[124a], T. Sarangi[172], E. Sarkisyan-Grinbaum[7], F. Sarri[122a,122b], G. Sartisohn[174], O. Sasaki[66], N. Sasao[68], I. Satsounkevitch[90], G. Sauvage[4], E. Sauvan[4], J.B. Sauvan[115], P. Savard[158,d], V. Savinov[123], D.O. Savu[29], L. Sawyer[24,l], D.H. Saxon[53], L.P. Says[33], C. Sbarra[19a], A. Sbrizzi[19a,19b], O. Scallon[93], D.A. Scannicchio[163], M. Scarcella[150], J. Schaarschmidt[115], P. Schacht[99], U. Schäfer[81], S. Schaepe[20], S. Schaetzel[58b], A.C. Schaffer[115], D. Schaile[98], R.D. Schamberger[148], A.G. Schamov[107], V. Scharf[58a], V.A. Schegelsky[121], D. Scheirich[87], M. Schernau[163], M.I. Scherzer[34], C. Schiavi[50a,50b], J. Schieck[98], M. Schioppa[36a,36b], S. Schlenker[29], J.L. Schlereth[5], E. Schmidt[48], K. Schmieden[20], C. Schmitt[81], S. Schmitt[58b], M. Schmitz[20], A. Schöning[58b], M. Schott[29], D. Schouten[159a], J. Schovancova[125], M. Schram[85], C. Schroeder[81], N. Schroer[58c], G. Schuler[29], M.J. Schultens[20], J. Schultes[174], H.-C. Schultz-Coulon[58a], H. Schulz[15], J.W. Schumacher[20], M. Schumacher[48], B.A. Schumm[137], Ph. Schune[136], C. Schwanenberger[82], A. Schwartzman[143], Ph. Schwemling[78], R. Schwienhorst[88], R. Schwierz[43], J. Schwindling[136], T. Schwindt[20], M. Schwoerer[4], W.G. Scott[129], J. Searcy[114], G. Sedov[41], E. Sedykh[121], E. Segura[11], S.C. Seidel[103], A. Seiden[137], F. Seifert[43], J.M. Seixas[23a], G. Sekhniaidze[102a], K.E. Selbach[45], D.M. Seliverstov[121], B. Sellden[146a], G. Sellers[73], M. Seman[144b], N. Semprini-Cesari[19a,19b], C. Serfon[98], L. Serin[115], L. Serkin[54], R. Seuster[99], H. Severini[111], M.E. Sevior[86], A. Sfyrla[29], E. Shabalina[54], M. Shamim[114], L.Y. Shan[32a], J.T. Shank[21], Q.T. Shao[86], M. Shapiro[14], P.B. Shatalov[95], L. Shaver[6], K. Shaw[164a,164c], D. Sherman[175], P. Sherwood[77], A. Shibata[108], H. Shichi[101], S. Shimizu[29], M. Shimojima[100], T. Shin[56], M. Shiyakova[65], A. Shmeleva[94], M.J. Shochet[30], D. Short[118], S. Shrestha[64], E. Shulga[96], M.A. Shupe[6], P. Sicho[125], A. Sidoti[132a], F. Siegert[48], Dj. Sijacki[12a], O. Silbert[171], J. Silva[124a], Y. Silver[153], D. Silverstein[143], S.B. Silverstein[146a], V. Simak[127], O. Simard[136], Lj. Simic[12a], S. Simion[115], B. Simmons[77], M. Simonyan[35], P. Sinervo[158], N.B. Sinev[114], V. Sipica[141], G. Siragusa[173], A. Sircar[24], A.N. Sisakyan[65], S.Yu. Sivoklokov[97], J. Sjölin[146a,146b], T.B. Sjursen[13], L.A. Skinnari[14], H.P. Skottowe[57], K. Skovpen[107], P. Skubic[111], N. Skvorodnev[22], M. Slater[17], T. Slavicek[127], K. Sliwa[161], J. Sloper[29], V. Smakhtin[171], B.H. Smart[45], S.Yu. Smirnov[96], Y. Smirnov[96], L.N. Smirnova[97], O. Smirnova[79], B.C. Smith[57], D. Smith[143], K.M. Smith[53], M. Smizanska[71], K. Smolek[127], A.A. Snesarev[94], S.W. Snow[82], J. Snow[111], J. Snuverink[105], S. Snyder[24], M. Soares[124a], R. Sobie[169,j], J. Sodomka[127], A. Soffer[153], C.A. Solans[167], M. Solar[127], J. Solc[127], E. Soldatov[96], U. Soldevila[167], E. Solfaroli Camillocci[132a,132b], A.A. Solodkov[128], O.V. Solovyanov[128], N. Soni[2], V. Sopko[127], B. Sopko[127], M. Sosebee[7], R. Soualah[164a,164c], A. Soukharev[107], S. Spagnolo[72a,72b], F. Spanò[76], R. Spighi[19a], G. Spigo[29], F. Spila[132a,132b], R. Spiwoks[29], M. Spousta[126], T. Spreitzer[158], B. Spurlock[7], R.D. St. Denis[53], J. Stahlman[120], R. Stamen[58a], E. Stanecka[38], R.W. Stanek[5], C. Stanescu[134a], S. Stapnes[117], E.A. Starchenko[128], J. Stark[55], P. Staroba[125], P. Starovoitov[91], A. Staude[98], P. Stavina[144a], G. Steele[53], P. Steinbach[43], P. Steinberg[24], I. Stekl[127], B. Stelzer[142], H.J. Stelzer[88], O. Stelzer-Chilton[159a], H. Stenzel[52], S. Stern[99], K. Stevenson[75], G.A. Stewart[29], J.A. Stillings[20], M.C. Stockton[85], K. Stoerig[48], G. Stoicea[25a], S. Stonjek[99], P. Strachota[126], A.R. Stradling[7], A. Straessner[43], J. Strandberg[147], S. Strandberg[146a,146b], A. Strandlie[117], M. Strang[109], E. Strauss[143], M. Strauss[111], P. Strizenec[144b], R. Ströhmer[173], D.M. Strom[114], J.A. Strong[76,*], R. Stroynowski[39], J. Strube[129], B. Stugu[13], I. Stumer[24,*], J. Stupak[148], P. Sturm[174], N.A. Styles[41], D.A. Soh[151,u], D. Su[143], H.S. Subramania[2], A. Succurro[11], Y. Sugaya[116], T. Sugimoto[101], C. Suhr[106], K. Suita[67], M. Suk[126], V.V. Sulin[94], S. Sultansoy[3d], T. Sumida[68], X. Sun[55], J.E. Sundermann[48], K. Suruliz[139], S. Sushkov[11], G. Susinno[36a,36b], M.R. Sutton[149], Y. Suzuki[66], Y. Suzuki[67], M. Svatos[125], Yu.M. Sviridov[128], S. Swedish[168], I. Sykora[144a], T. Sykora[126], B. Szeless[29], J. Sánchez[167], D. Ta[105], K. Tackmann[41], A. Taffard[163], R. Tafirout[159a], N. Taiblum[153], Y. Takahashi[101], H. Takai[24], R. Takashima[69], H. Takeda[67], T. Takeshita[140], Y. Takubo[66], M. Talby[83], A. Talyshev[107,f], M.C. Tamsett[24], J. Tanaka[155],

R. Tanaka[115], S. Tanaka[131], S. Tanaka[66], Y. Tanaka[100], A.J. Tanasijczuk[142], K. Tani[67], N. Tannoury[83], G.P. Tappern[29], S. Tapprogge[81], D. Tardif[158], S. Tarem[152], F. Tarrade[28], G.F. Tartarelli[89a], P. Tas[126], M. Tasevsky[125], E. Tassi[36a,36b], M. Tatarkhanov[14], Y. Tayalati[135d], C. Taylor[77], F.E. Taylor[92], G.N. Taylor[86], W. Taylor[159b], M. Teinturier[115], M. Teixeira Dias Castanheira[75], P. Teixeira-Dias[76], K.K. Temming[48], H. Ten Kate[29], P.K. Teng[151], S. Terada[66], K. Terashi[155], J. Terron[80], M. Testa[47], R.J. Teuscher[158,j], J. Thadome[174], J. Therhaag[20], T. Theveneaux-Pelzer[78], M. Thioye[175], S. Thoma[48], J.P. Thomas[17], E.N. Thompson[34], P.D. Thompson[17], P.D. Thompson[158], A.S. Thompson[53], L.A. Thomsen[35], E. Thomson[120], M. Thomson[27], R.P. Thun[87], F. Tian[34], M.J. Tibbetts[14], T. Tic[125], V.O. Tikhomirov[94], Y.A. Tikhonov[107,f], S Timoshenko[96], P. Tipton[175], F.J. Tique Aires Viegas[29], S. Tisserant[83], B. Toczek[37], T. Todorov[4], S. Todorova-Nova[161], B. Toggerson[163], J. Tojo[66], S. Tokár[144a], K. Tokunaga[67], K. Tokushuku[66], K. Tollefson[88], M. Tomoto[101], L. Tompkins[30], K. Toms[103], G. Tong[32a], A. Tonoyan[13], C. Topfel[16], N.D. Topilin[65], I. Torchiani[29], E. Torrence[114], H. Torres[78], E. Torró Pastor[167], J. Toth[83,aa], F. Touchard[83], D.R. Tovey[139], T. Trefzger[173], L. Tremblet[29], A. Tricoli[29], I.M. Trigger[159a], S. Trincaz-Duvoid[78], T.N. Trinh[78], M.F. Tripiana[70], W. Trischuk[158], A. Trivedi[24,z], B. Trocmé[55], C. Troncon[89a], M. Trottier-McDonald[142], M. Trzebinski[38], A. Trzupek[38], C. Tsarouchas[29], J.C.-L. Tseng[118], M. Tsiakiris[105], P.V. Tsiareshka[90], D. Tsionou[4,ae], G. Tsipolitis[9], V. Tsiskaridze[48], E.G. Tskhadadze[51a], I.I. Tsukerman[95], V. Tsulaia[14], J.-W. Tsung[20], S. Tsuno[66], D. Tsybychev[148], A. Tua[139], A. Tudorache[25a], V. Tudorache[25a], J.M. Tuggle[30], M. Turala[38], D. Turecek[127], I. Turk Cakir[3e], E. Turlay[105], R. Turra[89a,89b], P.M. Tuts[34], A. Tykhonov[74], M. Tylmad[146a,146b], M. Tyndel[129], G. Tzanakos[8], K. Uchida[20], I. Ueda[155], R. Ueno[28], M. Ugland[13], M. Uhlenbrock[20], M. Uhrmacher[54], F. Ukegawa[160], G. Unal[29], D.G. Underwood[5], A. Undrus[24], G. Unel[163], Y. Unno[66], D. Urbaniec[34], G. Usai[7], M. Uslenghi[119a,119b], L. Vacavant[83], V. Vacek[127], B. Vachon[85], S. Vahsen[14], J. Valenta[125], P. Valente[132a], S. Valentinetti[19a,19b], S. Valkar[126], E. Valladolid Gallego[167], S. Vallecorsa[152], J.A. Valls Ferrer[167], H. van der Graaf[105], E. van der Kraaij[105], R. Van Der Leeuw[105], E. van der Poel[105], D. van der Ster[29], N. van Eldik[84], P. van Gemmeren[5], Z. van Kesteren[105], I. van Vulpen[105], M. Vanadia[99], W. Vandelli[29], G. Vandoni[29], A. Vaniachine[5], P. Vankov[41], F. Vannucci[78], F. Varela Rodriguez[29], R. Vari[132a], E.W. Varnes[6], D. Varouchas[14], A. Vartapetian[7], K.E. Varvell[150], V.I. Vassilakopoulos[56], F. Vazeille[33], T. Vazquez Schroeder[54], G. Vegni[89a,89b], J.J. Veillet[115], C. Vellidis[8], F. Veloso[124a], R. Veness[29], S. Veneziano[132a], A. Ventura[72a,72b], D. Ventura[138], M. Venturi[48], N. Venturi[158], V. Vercesi[119a], M. Verducci[138], W. Verkerke[105], J.C. Vermeulen[105], A. Vest[43], M.C. Vetterli[142,d], I. Vichou[165], T. Vickey[145b,af], O.E. Vickey Boeriu[145b], G.H.A. Viehhauser[118], S. Viel[168], M. Villa[19a,19b], M. Villaplana Perez[167], E. Vilucchi[47], M.G. Vincter[28], E. Vinek[29], V.B. Vinogradov[65], M. Virchaux[136,*], J. Virzi[14], O. Vitells[171], M. Viti[41], I. Vivarelli[48], F. Vives Vaque[2], S. Vlachos[9], D. Vladoiu[98], M. Vlasak[127], N. Vlasov[20], A. Vogel[20], P. Vokac[127], G. Volpi[47], M. Volpi[86], G. Volpini[89a], H. von der Schmitt[99], J. von Loeben[99], H. von Radziewski[48], E. von Toerne[20], V. Vorobel[126], A.P. Vorobiev[128], V. Vorwerk[11], M. Vos[167], R. Voss[29], T.T. Voss[174], J.H. Vossebeld[73], N. Vranjes[136], M. Vranjes Milosavljevic[105], V. Vrba[125], M. Vreeswijk[105], T. Vu Anh[48], R. Vuillermet[29], I. Vukotic[115], W. Wagner[174], P. Wagner[120], H. Wahlen[174], J. Wakabayashi[101], J. Walbersloh[42], S. Walch[87], J. Walder[71], R. Walker[98], W. Walkowiak[141], R. Wall[175], P. Waller[73], C. Wang[44], H. Wang[172], H. Wang[32b,ag], J. Wang[151], J. Wang[55], J.C. Wang[138], R. Wang[103], S.M. Wang[151], A. Warburton[85], C.P. Ward[27], M. Warsinsky[48], P.M. Watkins[17], A.T. Watson[17], I.J. Watson[150], M.F. Watson[17], G. Watts[138], S. Watts[82], A.T. Waugh[150], B.M. Waugh[77], M. Weber[129], M.S. Weber[16], P. Weber[54], A.R. Weidberg[118], P. Weigell[99], J. Weingarten[54], C. Weiser[48], H. Wellenstein[22], P.S. Wells[29], T. Wenaus[24], D. Wendland[15], S. Wendler[123], Z. Weng[151,u], T. Wengler[29], S. Wenig[29], N. Wermes[20], M. Werner[48], P. Werner[29], M. Werth[163], M. Wessels[58a], C. Weydert[55], K. Whalen[28], S.J. Wheeler-Ellis[163], S.P. Whitaker[21], A. White[7], M.J. White[86], S.R. Whitehead[118], D. Whiteson[163], D. Whittington[61], F. Wicek[115], D. Wicke[174], F.J. Wickens[129], W. Wiedenmann[172], M. Wielers[129], P. Wienemann[20], C. Wiglesworth[75], L.A.M. Wiik-Fuchs[48], P.A. Wijeratne[77], A. Wildauer[167], M.A. Wildt[41,q], I. Wilhelm[126], H.G. Wilkens[29], J.Z. Will[98], E. Williams[34], H.H. Williams[120], W. Willis[34], S. Willocq[84], J.A. Wilson[17], M.G. Wilson[143], A. Wilson[87], I. Wingerter-Seez[4], S. Winkelmann[48], F. Winklmeier[29], M. Wittgen[143], M.W. Wolter[38], H. Wolters[124a,h], W.C. Wong[40], G. Wooden[87], B.K. Wosiek[38], J. Wotschack[29], M.J. Woudstra[84], K.W. Wozniak[38], K. Wraight[53], C. Wright[53], M. Wright[53], B. Wrona[73], S.L. Wu[172], X. Wu[49], Y. Wu[32b,ah], E. Wulf[34], R. Wunstorf[42], B.M. Wynne[45], S. Xella[35], M. Xiao[136], S. Xie[48], Y. Xie[32a], C. Xu[32b,w], D. Xu[139], G. Xu[32a], B. Yabsley[150], S. Yacoob[145b], M. Yamada[66], H. Yamaguchi[155], A. Yamamoto[66], K. Yamamoto[64], S. Yamamoto[155], T. Yamamura[155], T. Yamanaka[155], J. Yamaoka[44], T. Yamazaki[155], Y. Yamazaki[67], Z. Yan[21], H. Yang[87], U.K. Yang[82], Y. Yang[61], Y. Yang[32a], Z. Yang[146a,146b], S. Yanush[91], Y. Yao[14], Y. Yasu[66], G.V. Ybeles Smit[130], J. Ye[39], S. Ye[24], M. Yilmaz[3c], R. Yoosoofmiya[123], K. Yorita[170], R. Yoshida[5], C. Young[143], S. Youssef[21], D. Yu[24], J. Yu[7], J. Yu[112], L. Yuan[32a,ai], A. Yurkewicz[106], B. Zabinski[38], V.G. Zaets[128], R. Zaidan[63], A.M. Zaitsev[128], Z. Zajacova[29], L. Zanello[132a,132b], A. Zaytsev[107], C. Zeitnitz[174], M. Zeller[175], M. Zeman[125], A. Zemla[38], C. Zendler[20], O. Zenin[128], T. Ženiš[144a], Z. Zinonos[122a,122b], S. Zenz[14], D. Zerwas[115], G. Zevi della Porta[57], Z. Zhan[32d], D. Zhang[32b,ag], H. Zhang[88], J. Zhang[5], X. Zhang[32d], Z. Zhang[115], L. Zhao[108], T. Zhao[138], Z. Zhao[32b], A. Zhemchugov[65], S. Zheng[32a], J. Zhong[118], B. Zhou[87], N. Zhou[163], Y. Zhou[151], C.G. Zhu[32d], H. Zhu[41], J. Zhu[87], Y. Zhu[32b], X. Zhuang[98], V. Zhuravlov[99], D. Zieminska[61], R. Zimmermann[20], S. Zim-

mermann[20], S. Zimmermann[48], M. Ziolkowski[141], R. Zitoun[4], L. Živković[34], V.V. Zmouchko[128,*], G. Zobernig[172], A. Zoccoli[19a,19b], Y. Zolnierowski[4], A. Zsenei[29], M. zur Nedden[15], V. Zutshi[106], L. Zwalinski[29]

[1] University at Albany, Albany NY, United States of America

[2] Department of Physics, University of Alberta, Edmonton AB, Canada

[3] (a) Department of Physics, Ankara University, Ankara; (b) Department of Physics, Dumlupinar University, Kutahya; (c) Department of Physics, Gazi University, Ankara; (d) Division of Physics, TOBB University of Economics and Technology, Ankara; (e) Turkish Atomic Energy Authority, Ankara, Turkey

[4] LAPP, CNRS/IN2P3 and Université de Savoie, Annecy-le-Vieux, France

[5] High Energy Physics Division, Argonne National Laboratory, Argonne IL, United States of America

[6] Department of Physics, University of Arizona, Tucson AZ, United States of America

[7] Department of Physics, The University of Texas at Arlington, Arlington TX, United States of America

[8] Physics Department, University of Athens, Athens, Greece

[9] Physics Department, National Technical University of Athens, Zografou, Greece

[10] Institute of Physics, Azerbaijan Academy of Sciences, Baku, Azerbaijan

[11] Institut de Física d'Altes Energies and Departament de Física de la Universitat Autònoma de Barcelona and ICREA, Barcelona, Spain

[12] (a) Institute of Physics, University of Belgrade, Belgrade; (b) Vinca Institute of Nuclear Sciences, University of Belgrade, Belgrade, Serbia

[13] Department for Physics and Technology, University of Bergen, Bergen, Norway

[14] Physics Division, Lawrence Berkeley National Laboratory and University of California, Berkeley CA, United States of America

[15] Department of Physics, Humboldt University, Berlin, Germany

[16] Albert Einstein Center for Fundamental Physics and Laboratory for High Energy Physics, University of Bern, Bern, Switzerland

[17] School of Physics and Astronomy, University of Birmingham, Birmingham, United Kingdom

[18] (a) Department of Physics, Bogazici University, Istanbul; (b) Division of Physics, Dogus University, Istanbul; (c) Department of Physics Engineering, Gaziantep University, Gaziantep; (d) Department of Physics, Istanbul Technical University, Istanbul, Turkey

[19] (a) INFN Sezione di Bologna; (b) Dipartimento di Fisica, Università di Bologna, Bologna, Italy

[20] Physikalisches Institut, University of Bonn, Bonn, Germany

[21] Department of Physics, Boston University, Boston MA, United States of America

[22] Department of Physics, Brandeis University, Waltham MA, United States of America

[23] (a) Universidade Federal do Rio De Janeiro COPPE/EE/IF, Rio de Janeiro; (b) Federal University of Juiz de Fora (UFJF), Juiz de Fora; (c) Federal University of Sao Joao del Rei (UFSJ), Sao Joao del Rei; (d) Instituto de Fisica, Universidade de Sao Paulo, Sao Paulo, Brazil

[24] Physics Department, Brookhaven National Laboratory, Upton NY, United States of America

[25] (a) National Institute of Physics and Nuclear Engineering, Bucharest; (b) University Politehnica Bucharest, Bucharest; (c) West University in Timisoara, Timisoara, Romania

[26] Departamento de Física, Universidad de Buenos Aires, Buenos Aires, Argentina

[27] Cavendish Laboratory, University of Cambridge, Cambridge, United Kingdom

[28] Department of Physics, Carleton University, Ottawa ON, Canada

[29] CERN, Geneva, Switzerland

[30] Enrico Fermi Institute, University of Chicago, Chicago IL, United States of America

[31] (a) Departamento de Fisica, Pontificia Universidad Católica de Chile, Santiago; (b) Departamento de Física, Universidad Técnica Federico Santa María, Valparaíso, Chile

[32] (a) Institute of High Energy Physics, Chinese Academy of Sciences, Beijing; (b) Department of Modern Physics, University of Science and Technology of China, Anhui; (c) Department of Physics, Nanjing University, Jiangsu; (d) School of Physics, Shandong University, Shandong, China

[33] Laboratoire de Physique Corpusculaire, Clermont Université and Université Blaise Pascal and CNRS/IN2P3, Aubiere Cedex, France

[34] Nevis Laboratory, Columbia University, Irvington NY, United States of America

[35] Niels Bohr Institute, University of Copenhagen, Kobenhavn, Denmark

[36] (a) INFN Gruppo Collegato di Cosenza; (b) Dipartimento di Fisica, Università della Calabria, Arcavata di Rende, Italy

[37]AGH University of Science and Technology, Faculty of Physics and Applied Computer Science, Krakow, Poland

[38]The Henryk Niewodniczanski Institute of Nuclear Physics, Polish Academy of Sciences, Krakow, Poland

[39]Physics Department, Southern Methodist University, Dallas TX, United States of America

[40]Physics Department, University of Texas at Dallas, Richardson TX, United States of America

[41]DESY, Hamburg and Zeuthen, Germany

[42]Institut für Experimentelle Physik IV, Technische Universität Dortmund, Dortmund, Germany

[43]Institut für Kern- und Teilchenphysik, Technical University Dresden, Dresden, Germany

[44]Department of Physics, Duke University, Durham NC, United States of America

[45]SUPA - School of Physics and Astronomy, University of Edinburgh, Edinburgh, United Kingdom

[46]Fachhochschule Wiener Neustadt, Johannes Gutenbergstrasse 3, 2700 Wiener Neustadt, Austria

[47]INFN Laboratori Nazionali di Frascati, Frascati, Italy

[48]Fakultät für Mathematik und Physik, Albert-Ludwigs-Universität, Freiburg i.Br., Germany

[49]Section de Physique, Université de Genève, Geneva, Switzerland

[50](a)INFN Sezione di Genova; (b)Dipartimento di Fisica, Università di Genova, Genova, Italy

[51](a)E.Andronikashvili Institute of Physics, Tbilisi State University, Tbilisi; (b)High Energy Physics Institute, Tbilisi State University, Tbilisi, Georgia

[52]II Physikalisches Institut, Justus-Liebig-Universität Giessen, Giessen, Germany

[53]SUPA - School of Physics and Astronomy, University of Glasgow, Glasgow, United Kingdom

[54]II Physikalisches Institut, Georg-August-Universität, Göttingen, Germany

[55]Laboratoire de Physique Subatomique et de Cosmologie, Université Joseph Fourier and CNRS/IN2P3 and Institut National Polytechnique de Grenoble, Grenoble, France

[56]Department of Physics, Hampton University, Hampton VA, United States of America

[57]Laboratory for Particle Physics and Cosmology, Harvard University, Cambridge MA, United States of America

[58](a)Kirchhoff-Institut für Physik, Ruprecht-Karls-Universität Heidelberg, Heidelberg; (b)Physikalisches Institut, Ruprecht-Karls-Universität Heidelberg, Heidelberg; (c)ZITI Institut für technische Informatik, Ruprecht-Karls-Universität Heidelberg, Mannheim, Germany

[59]Faculty of Science, Hiroshima University, Hiroshima, Japan

[60]Faculty of Applied Information Science, Hiroshima Institute of Technology, Hiroshima, Japan

[61]Department of Physics, Indiana University, Bloomington IN, United States of America

[62]Institut für Astro- und Teilchenphysik, Leopold-Franzens-Universität, Innsbruck, Austria

[63]University of Iowa, Iowa City IA, United States of America

[64]Department of Physics and Astronomy, Iowa State University, Ames IA, United States of America

[65]Joint Institute for Nuclear Research, JINR Dubna, Dubna, Russia

[66]KEK, High Energy Accelerator Research Organization, Tsukuba, Japan

[67]Graduate School of Science, Kobe University, Kobe, Japan

[68]Faculty of Science, Kyoto University, Kyoto, Japan

[69]Kyoto University of Education, Kyoto, Japan

[70]Instituto de Física La Plata, Universidad Nacional de La Plata and CONICET, La Plata, Argentina

[71]Physics Department, Lancaster University, Lancaster, United Kingdom

[72](a)INFN Sezione di Lecce; (b)Dipartimento di Fisica, Università del Salento, Lecce, Italy

[73]Oliver Lodge Laboratory, University of Liverpool, Liverpool, United Kingdom

[74]Department of Physics, Jožef Stefan Institute and University of Ljubljana, Ljubljana, Slovenia

[75]School of Physics and Astronomy, Queen Mary University of London, London, United Kingdom

[76]Department of Physics, Royal Holloway University of London, Surrey, United Kingdom

[77]Department of Physics and Astronomy, University College London, London, United Kingdom

[78]Laboratoire de Physique Nucléaire et de Hautes Energies, UPMC and Université Paris-Diderot and CNRS/IN2P3, Paris, France

[79]Fysiska institutionen, Lunds universitet, Lund, Sweden

[80]Departamento de Fisica Teorica C-15, Universidad Autonoma de Madrid, Madrid, Spain

[81]Institut für Physik, Universität Mainz, Mainz, Germany

[82]School of Physics and Astronomy, University of Manchester, Manchester, United Kingdom

[83]CPPM, Aix-Marseille Université and CNRS/IN2P3, Marseille, France

[84]Department of Physics, University of Massachusetts, Amherst MA, United States of America

[85] Department of Physics, McGill University, Montreal QC, Canada

[86] School of Physics, University of Melbourne, Victoria, Australia

[87] Department of Physics, The University of Michigan, Ann Arbor MI, United States of America

[88] Department of Physics and Astronomy, Michigan State University, East Lansing MI, United States of America

[89] (a) INFN Sezione di Milano; (b) Dipartimento di Fisica, Università di Milano, Milano, Italy

[90] B.I. Stepanov Institute of Physics, National Academy of Sciences of Belarus, Minsk, Republic of Belarus

[91] National Scientific and Educational Centre for Particle and High Energy Physics, Minsk, Republic of Belarus

[92] Department of Physics, Massachusetts Institute of Technology, Cambridge MA, United States of America

[93] Group of Particle Physics, University of Montreal, Montreal QC, Canada

[94] P.N. Lebedev Institute of Physics, Academy of Sciences, Moscow, Russia

[95] Institute for Theoretical and Experimental Physics (ITEP), Moscow, Russia

[96] Moscow Engineering and Physics Institute (MEPhI), Moscow, Russia

[97] Skobeltsyn Institute of Nuclear Physics, Lomonosov Moscow State University, Moscow, Russia

[98] Fakultät für Physik, Ludwig-Maximilians-Universität München, München, Germany

[99] Max-Planck-Institut für Physik (Werner-Heisenberg-Institut), München, Germany

[100] Nagasaki Institute of Applied Science, Nagasaki, Japan

[101] Graduate School of Science, Nagoya University, Nagoya, Japan

[102] (a) INFN Sezione di Napoli; (b) Dipartimento di Scienze Fisiche, Università di Napoli, Napoli, Italy

[103] Department of Physics and Astronomy, University of New Mexico, Albuquerque NM, United States of America

[104] Institute for Mathematics, Astrophysics and Particle Physics, Radboud University Nijmegen/Nikhef, Nijmegen, Netherlands

[105] Nikhef National Institute for Subatomic Physics and University of Amsterdam, Amsterdam, Netherlands

[106] Department of Physics, Northern Illinois University, DeKalb IL, United States of America

[107] Budker Institute of Nuclear Physics, SB RAS, Novosibirsk, Russia

[108] Department of Physics, New York University, New York NY, United States of America

[109] Ohio State University, Columbus OH, United States of America

[110] Faculty of Science, Okayama University, Okayama, Japan

[111] Homer L. Dodge Department of Physics and Astronomy, University of Oklahoma, Norman OK, United States of America

[112] Department of Physics, Oklahoma State University, Stillwater OK, United States of America

[113] Palacký University, RCPTM, Olomouc, Czech Republic

[114] Center for High Energy Physics, University of Oregon, Eugene OR, United States of America

[115] LAL, Univ. Paris-Sud and CNRS/IN2P3, Orsay, France

[116] Graduate School of Science, Osaka University, Osaka, Japan

[117] Department of Physics, University of Oslo, Oslo, Norway

[118] Department of Physics, Oxford University, Oxford, United Kingdom

[119] (a) INFN Sezione di Pavia; (b) Dipartimento di Fisica, Università di Pavia, Pavia, Italy

[120] Department of Physics, University of Pennsylvania, Philadelphia PA, United States of America

[121] Petersburg Nuclear Physics Institute, Gatchina, Russia

[122] (a) INFN Sezione di Pisa; (b) Dipartimento di Fisica E. Fermi, Università di Pisa, Pisa, Italy

[123] Department of Physics and Astronomy, University of Pittsburgh, Pittsburgh PA, United States of America

[124] (a) Laboratorio de Instrumentacao e Fisica Experimental de Particulas - LIP, Lisboa, Portugal; (b) Departamento de Fisica Teorica y del Cosmos and CAFPE, Universidad de Granada, Granada, Spain

[125] Institute of Physics, Academy of Sciences of the Czech Republic, Praha, Czech Republic

[126] Faculty of Mathematics and Physics, Charles University in Prague, Praha, Czech Republic

[127] Czech Technical University in Prague, Praha, Czech Republic

[128] State Research Center Institute for High Energy Physics, Protvino, Russia

[129] Particle Physics Department, Rutherford Appleton Laboratory, Didcot, United Kingdom

[130] Physics Department, University of Regina, Regina SK, Canada

[131] Ritsumeikan University, Kusatsu, Shiga, Japan

[132] (a) INFN Sezione di Roma I; (b) Dipartimento di Fisica, Università La Sapienza, Roma, Italy

[133] (a) INFN Sezione di Roma Tor Vergata; (b) Dipartimento di Fisica, Università di Roma Tor Vergata, Roma, Italy

[134] (a) INFN Sezione di Roma Tre; (b) Dipartimento di Fisica, Università Roma Tre, Roma, Italy

[135] (a)Faculté des Sciences Ain Chock, Réseau Universitaire de Physique des Hautes Energies - Université Hassan II, Casablanca; (b)Centre National de l'Energie des Sciences Techniques Nucleaires, Rabat; (c)Faculté des Sciences Semlalia, Université Cadi Ayyad, LPHEA-Marrakech; (d)Faculté des Sciences, Université Mohamed Premier and LPTPM, Oujda; (e)Faculté des Sciences, Université Mohammed V- Agdal, Rabat, Morocco

[136] DSM/IRFU (Institut de Recherches sur les Lois Fondamentales de l'Univers), CEA Saclay (Commissariat a l'Energie Atomique), Gif-sur-Yvette, France

[137] Santa Cruz Institute for Particle Physics, University of California Santa Cruz, Santa Cruz CA, United States of America

[138] Department of Physics, University of Washington, Seattle WA, United States of America

[139] Department of Physics and Astronomy, University of Sheffield, Sheffield, United Kingdom

[140] Department of Physics, Shinshu University, Nagano, Japan

[141] Fachbereich Physik, Universität Siegen, Siegen, Germany

[142] Department of Physics, Simon Fraser University, Burnaby BC, Canada

[143] SLAC National Accelerator Laboratory, Stanford CA, United States of America

[144] (a)Faculty of Mathematics, Physics & Informatics, Comenius University, Bratislava; (b)Department of Subnuclear Physics, Institute of Experimental Physics of the Slovak Academy of Sciences, Kosice, Slovak Republic

[145] (a)Department of Physics, University of Johannesburg, Johannesburg; (b)School of Physics, University of the Witwatersrand, Johannesburg, South Africa

[146] (a)Department of Physics, Stockholm University; (b)The Oskar Klein Centre, Stockholm, Sweden

[147] Physics Department, Royal Institute of Technology, Stockholm, Sweden

[148] Departments of Physics & Astronomy and Chemistry, Stony Brook University, Stony Brook NY, United States of America

[149] Department of Physics and Astronomy, University of Sussex, Brighton, United Kingdom

[150] School of Physics, University of Sydney, Sydney, Australia

[151] Institute of Physics, Academia Sinica, Taipei, Taiwan

[152] Department of Physics, Technion: Israel Inst. of Technology, Haifa, Israel

[153] Raymond and Beverly Sackler School of Physics and Astronomy, Tel Aviv University, Tel Aviv, Israel

[154] Department of Physics, Aristotle University of Thessaloniki, Thessaloniki, Greece

[155] International Center for Elementary Particle Physics and Department of Physics, The University of Tokyo, Tokyo, Japan

[156] Graduate School of Science and Technology, Tokyo Metropolitan University, Tokyo, Japan

[157] Department of Physics, Tokyo Institute of Technology, Tokyo, Japan

[158] Department of Physics, University of Toronto, Toronto ON, Canada

[159] (a)TRIUMF, Vancouver BC; (b)Department of Physics and Astronomy, York University, Toronto ON, Canada

[160] Institute of Pure and Applied Sciences, University of Tsukuba, 1-1-1 Tennodai, Tsukuba, Ibaraki 305-8571, Japan

[161] Science and Technology Center, Tufts University, Medford MA, United States of America

[162] Centro de Investigaciones, Universidad Antonio Narino, Bogota, Colombia

[163] Department of Physics and Astronomy, University of California Irvine, Irvine CA, United States of America

[164] (a)INFN Gruppo Collegato di Udine, Udine; (b)ICTP, Trieste; (c)Dipartimento di Chimica, Fisica e Ambiente, Università di Udine, Udine, Italy

[165] Department of Physics, University of Illinois, Urbana IL, United States of America

[166] Department of Physics and Astronomy, University of Uppsala, Uppsala, Sweden

[167] Instituto de Física Corpuscular (IFIC) and Departamento de Física Atómica, Molecular y Nuclear and Departamento de Ingeniería Electrónica and Instituto de Microelectrónica de Barcelona (IMB-CNM), University of Valencia and CSIC, Valencia, Spain

[168] Department of Physics, University of British Columbia, Vancouver BC, Canada

[169] Department of Physics and Astronomy, University of Victoria, Victoria BC, Canada

[170] Waseda University, Tokyo, Japan

[171] Department of Particle Physics, The Weizmann Institute of Science, Rehovot, Israel

[172] Department of Physics, University of Wisconsin, Madison WI, United States of America

[173] Fakultät für Physik und Astronomie, Julius-Maximilians-Universität, Würzburg, Germany

[174] Fachbereich C Physik, Bergische Universität Wuppertal, Wuppertal, Germany

[175] Department of Physics, Yale University, New Haven CT, United States of America

[176] Yerevan Physics Institute, Yerevan, Armenia

[177] Domaine scientifique de la Doua, Centre de Calcul CNRS/IN2P3, Villeurbanne Cedex, France

[a] Also at Laboratorio de Instrumentacao e Fisica Experimental de Particulas - LIP, Lisboa, Portugal

[b] Also at Faculdade de Ciencias and CFNUL, Universidade de Lisboa, Lisboa, Portugal

[c] Also at Particle Physics Department, Rutherford Appleton Laboratory, Didcot, United Kingdom

[d] Also at TRIUMF, Vancouver BC, Canada

[e] Also at Department of Physics, California State University, Fresno CA, United States of America

[f] Also at Novosibirsk State University, Novosibirsk, Russia

[g] Also at Fermilab, Batavia IL, United States of America

[h] Also at Department of Physics, University of Coimbra, Coimbra, Portugal

[i] Also at Università di Napoli Parthenope, Napoli, Italy

[j] Also at Institute of Particle Physics (IPP), Canada

[k] Also at Department of Physics, Middle East Technical University, Ankara, Turkey

[l] Also at Louisiana Tech University, Ruston LA, United States of America

[m] Also at Department of Physics and Astronomy, University College London, London, United Kingdom

[n] Also at Group of Particle Physics, University of Montreal, Montreal QC, Canada

[o] Also at Department of Physics, University of Cape Town, Cape Town, South Africa

[p] Also at Institute of Physics, Azerbaijan Academy of Sciences, Baku, Azerbaijan

[q] Also at Institut für Experimentalphysik, Universität Hamburg, Hamburg, Germany

[r] Also at Manhattan College, New York NY, United States of America

[s] Also at School of Physics, Shandong University, Shandong, China

[t] Also at CPPM, Aix-Marseille Université and CNRS/IN2P3, Marseille, France

[u] Also at School of Physics and Engineering, Sun Yat-sen University, Guanzhou, China

[v] Also at Academia Sinica Grid Computing, Institute of Physics, Academia Sinica, Taipei, Taiwan

[w] Also at DSM/IRFU (Institut de Recherches sur les Lois Fondamentales de l'Univers), CEA Saclay (Commissariat a l'Energie Atomique), Gif-sur-Yvette, France

[x] Also at Section de Physique, Université de Genève, Geneva, Switzerland

[y] Also at Departamento de Fisica, Universidade de Minho, Braga, Portugal

[z] Also at Department of Physics and Astronomy, University of South Carolina, Columbia SC, United States of America

[aa] Also at Institute for Particle and Nuclear Physics, Wigner Research Centre for Physics, Budapest, Hungary

[ab] Also at California Institute of Technology, Pasadena CA, United States of America

[ac] Also at Institute of Physics, Jagiellonian University, Krakow, Poland

[ad] Also at LAL, Univ. Paris-Sud and CNRS/IN2P3, Orsay, France

[ae] Also at Department of Physics and Astronomy, University of Sheffield, Sheffield, United Kingdom

[af] Also at Department of Physics, Oxford University, Oxford, United Kingdom

[ag] Also at Institute of Physics, Academia Sinica, Taipei, Taiwan

[ah] Also at Department of Physics, The University of Michigan, Ann Arbor MI, United States of America

[ai] Also at Laboratoire de Physique Nucléaire et de Hautes Energies, UPMC and Université Paris-Diderot and CNRS/IN2P3, Paris, France

[*] Deceased